

# BIT Numerical Mathematics

## Robin-to-Robin transparent boundary conditions for the computation of guided modes in photonic crystal wave-guides

--Manuscript Draft--

<b>Manuscript Number:</b>	
<b>Full Title:</b>	Robin-to-Robin transparent boundary conditions for the computation of guided modes in photonic crystal wave-guides
<b>Article Type:</b>	S.I. :Oberwolfach Conference on Computational Electromagnetics and Acoustis
<b>Corresponding Author:</b>	Dirk Klindworth TU Berlin GERMANY
<b>Corresponding Author Secondary Information:</b>	
<b>Corresponding Author's Institution:</b>	TU Berlin
<b>Corresponding Author's Secondary Institution:</b>	
<b>First Author:</b>	Sonia Fliss
<b>First Author Secondary Information:</b>	
<b>Order of Authors:</b>	Sonia Fliss Dirk Klindworth Kersten Schmidt
<b>Order of Authors Secondary Information:</b>	
<b>Abstract:</b>	<p>The efficient and reliable computation of guided modes in photonic crystal wave-guides is of great importance for designing optical devices. Transparent boundary conditions based on Dirichlet-to-Neumann operators allow for an exact computation of well-confined modes and modes close to the band edge in the sense that no modelling error is introduced. The well-known super-cell method, on the other hand, introduces a modelling error which may become prohibitively large for guided modes that are not well-confined. The Dirichlet-to-Neumann transparent boundary conditions are, however, not applicable for all frequencies as they are not uniquely defined and their computation is unstable for a countable set of frequencies that correspond to so called Dirichlet eigenvalues. In this work we describe how to overcome this theoretical difficulty introducing Robin-to-Robin transparent boundary conditions whose construction do not exhibit those forbidden frequencies. They seem, hence, well suited for an exact and reliable computation of guided modes in photonic crystal wave-guides.</p>
<b>Suggested Reviewers:</b>	

**BIT manuscript No.**

(will be inserted by the editor)

---

# Robin-to-Robin transparent boundary conditions for the computation of guided modes in photonic crystal wave-guides

Sonia Fliss · Dirk Klindworth · Kersten Schmidt

Received: date / Accepted: date

**Abstract** The efficient and reliable computation of guided modes in photonic crystal wave-guides is of great importance for designing optical devices. Transparent boundary conditions based on Dirichlet-to-Neumann operators allow for an exact computation of well-confined modes and modes close to the band edge in the sense that no modelling error is introduced. The well-known super-cell method, on the other hand, introduces a modelling error which may become prohibitively large for guided modes that are not well-confined. The Dirichlet-to-Neumann transparent boundary conditions are, however, not applicable for all frequencies as they are not uniquely defined and their computation is unstable for a countable set of frequencies that correspond to so called Dirichlet eigenvalues. In this work we describe how to overcome this theoretical difficulty introducing Robin-to-Robin transparent boundary conditions whose construction do not exhibit those forbidden frequencies. They seem, hence, well suited for an exact and reliable computation of guided modes in photonic crystal wave-guides.

**Keywords** Robin-to-Robin map · photonic crystal wave-guide · surface modes · high-order FEM · non-linear eigenvalue problem

**Mathematics Subject Classification (2000)** 35P30 · 35Q61 · 65N30 · 65Z05 · 78-04 · 78M10

---

S. Fliss

Laboratoire POEMS, UMR 7231 CNRS/ENSTA/INRIA, ENSTA ParisTech, Paris, France

E-mail: [sonia.fliss@ensta-paristech.fr](mailto:sonia.fliss@ensta-paristech.fr)

D. Klindworth

DFG Research Center MATHEON, TU Berlin, Berlin, Germany

E-mail: [dirk.klindworth@math.tu-berlin.de](mailto:dirk.klindworth@math.tu-berlin.de)

K. Schmidt

DFG Research Center MATHEON, TU Berlin, Berlin, Germany

E-mail: [kersten.schmidt@math.tu-berlin.de](mailto:kersten.schmidt@math.tu-berlin.de)

1  
2  
3  
4  
5  
6  
7  
8  
9  
10  
11  
12  
13  
14  
15  
16  
17  
18  
19  
20  
21  
22  
23  
24  
25  
26  
27  
28  
29  
30  
31  
32  
33  
34  
35  
36  
37  
38  
39  
40  
41  
42  
43  
44  
45  
46  
47  
48  
49  
50  
51  
52  
53  
54  
55  
56  
57  
58  
59  
60  
61  
62  
63  
64  
65

## 1 Introduction

Transparent boundary conditions for 2D periodic media have been studied extensively in the last years, see for example [11,7,6,2,1]. These transparent boundary conditions are based on Dirichlet-to-Neumann (DtN) maps, and are applied to scattering problems at local defects in 2D periodic media, *e.g.* a 2D photonic crystal (PhC) with a local perturbation of its holes or rods respectively. Recently, this DtN approach was rigorously extended to the band structure calculation of 2D PhC waveguides [5]. The numerical realization of these DtN transparent boundary conditions with the high-order finite element method (FEM) was shown in [13]. The numerical solution of the resulting non-linear eigenvalue problem was also addressed in [13].

The DtN maps are defined via Dirichlet problems in infinite half-strips and their computation requires the solution of local Dirichlet problems in a unit cell of the periodic medium. By solving these Dirichlet problems the band gaps of the periodic medium can be deduced. Band gaps are frequency intervals for which monochromatic waves cannot propagate in the periodic medium. Due to the perturbation, authorized frequencies may appear inside these forbidden intervals of frequencies. The modes associated to these authorized frequencies are the so called *guided modes* which propagate along the line defect of the PhC wave-guide and vanish inside the periodic media. In order to compute guided modes, we therefore aim to define and compute the DtN maps at all frequencies in the band gaps. However – and this is the main disadvantage of the DtN approach — both, the Dirichlet problems in the infinite half-strips as well as the local Dirichlet cell problems, have frequency eigenvalues, so called *global* and *local Dirichlet eigenvalues* respectively. For these countable sets of Dirichlet eigenvalues the Dirichlet problems in the infinite half-strips and the Dirichlet problems in the unit cell, respectively, are not well-posed [11], and hence, the DtN maps are not well-defined at global Dirichlet eigenvalues and their computation is not stable at local Dirichlet eigenvalues. This disadvantage can be overcome by introducing Robin-to-Robin (RtR) maps instead of DtN maps [4,8]. The RtR maps are well defined at all frequencies outside the essential spectrum.

The computation of these RtR maps is, however, more involved than the computation of the DtN maps. This explains the small number of publications on this method. In this paper we aim to explain the construction of these RtR transparent boundary conditions and elaborate on their numerical realization. We shall also introduce DtN maps which are based on local Robin cell problems and which are thus also computable at Dirichlet eigenvalues of the local cell problems. However, these DtN maps remain ill-posed at Dirichlet eigenvalues of the infinite half-strip problems. The application that we will deal with are band structure calculations of 2D PhC wave-guides and the computation of surface modes at the boundary of a periodic medium with homogeneous Dirichlet boundary conditions.

This paper is organized as follows: in Section 2 we will introduce the model problems. The definition, characterization and discretization of the RtR operators is presented in Section 3. In Section 4 we transform the model problems, which are posed on unbounded domains, to non-linear problems on bounded domains using the previously defined RtR operators. The discretization and numerical solution of these non-linear eigenvalue problems is also shown in Section 4. Numerical results

of our model problems, including a comparison of the results when employing RtR and DtN maps, are presented in Section 5. Finally, we will give concluding remarks in Section 6.

## 2 Model problem

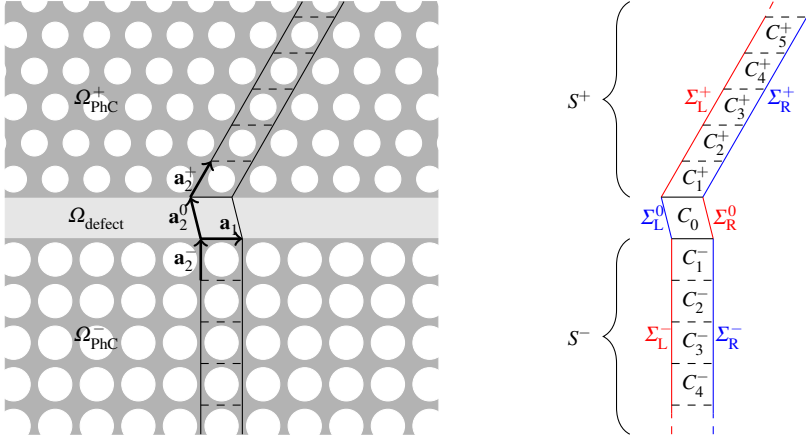
### 2.1 The geometry of photonic crystals and photonic crystal wave-guides

2D PhCs are generally described by a periodic permittivity  $\varepsilon_{\text{PhC}} : \mathbb{R}^2 \rightarrow \mathbb{R}^+ \setminus \{0\}$ , which is bounded from below and above, and which satisfies the periodicity conditions  $\varepsilon_{\text{PhC}}(\mathbf{x} + \mathbf{a}_i) = \varepsilon_{\text{PhC}}(\mathbf{x})$ ,  $i = 1, 2$ , where — without loss of generality — we assume that  $\mathbf{a}_1 = a_1 (1, 0)^T$ ,  $a_1 > 0$ . In most applications,  $\varepsilon_{\text{PhC}}$  takes some constant value in the holes or rods and some other constant value in the bulk.

For the permittivity  $\varepsilon_{\text{wg}} : \mathbb{R}^2 \rightarrow \mathbb{R}^+ \setminus \{0\}$  of a 2D PhC wave-guide with line defect of height  $a_{22}^0 > 0$  we choose the piecewise definition

$$\varepsilon_{\text{wg}}(\mathbf{x}) = \begin{cases} \varepsilon_{\text{PhC}}^-(\mathbf{x}), & \text{if } \mathbf{x} \in \Omega_{\text{PhC}}^- := \mathbb{R} \times ]-\infty, -a_{22}^0/2[, \\ \varepsilon_{\text{defect}}(\mathbf{x}), & \text{if } \mathbf{x} \in \Omega_{\text{defect}} := \mathbb{R} \times ]-a_{22}^0/2, a_{22}^0/2[, \\ \varepsilon_{\text{PhC}}^+(\mathbf{x}), & \text{if } \mathbf{x} \in \Omega_{\text{PhC}}^+ := \mathbb{R} \times ]a_{22}^0/2, \infty[, \end{cases}$$

where  $\mathbf{a}_1^- = \mathbf{a}_1^+ = \mathbf{a}_1 = a_1 (1, 0)^T$  and  $\mathbf{a}_2^0 = (a_{21}^0, a_{22}^0)^T$ , see Figure 2.1(a).



(a) Sketch of the domain  $\Omega_{\text{wg}} = \Omega_{\text{PhC}}^+ \cup \Omega_{\text{defect}} \cup \Omega_{\text{PhC}}^-$  of a PhC wave-guide with homogeneous line defect, PhC of square lattice below the defect, and PhC of hexagonal lattice on top of the defect.

(b) Sketch of the periodicity strip  $S = S^+ \cup C_0 \cup S^-$  of the PhC wave-guide presented on the left, its unit cells and left and right boundaries.

**Fig. 2.1** Sketch of a PhC wave-guide and its periodicity strip  $S$ .

## 2.2 Model problem of finding guided modes

In PhC wave-guides there exist guided modes, also called trapped modes, which are eigensolutions of the time-harmonic Maxwell's equations and which propagate along the line defect (*i. e.* along the  $x_1$ -axis) while decaying in the directions orthogonal to the line defect (*i. e.* along the  $x_2$ -axis).

In 2D the time-harmonic Maxwell's equations decouple into a transverse magnetic (TM) and a transverse electric (TE) mode that satisfy a 2D linear Helmholtz equation [10]. For simplicity let us consider the TM-mode, for which

$$-\Delta E(\mathbf{x}) - \omega^2 \varepsilon(\mathbf{x}) E(\mathbf{x}) = 0, \quad \mathbf{x} \in \mathbb{R}^2,$$

defines the electric field  $E$  in  $x_3$ -direction.

All results of this article can easily be transferred to the TE-mode for which the magnetic field  $H$  in  $x_3$ -direction satisfies

$$-\nabla \cdot \frac{1}{\varepsilon(\mathbf{x})} \nabla H(\mathbf{x}) - \omega^2 H(\mathbf{x}) = 0, \quad \mathbf{x} \in \mathbb{R}^2.$$

A guided mode is, by definition, a non trivial solution of

$$-\Delta e_k(\mathbf{x}) - \omega^2 \varepsilon(\mathbf{x}) e_k(\mathbf{x}) = 0 \quad (2.1a)$$

in the infinite strip  $S = S^+ \cup C_0 \cup S^- \subset \mathbb{R}^2$ , *c.f.* Figure 2.1, which satisfies quasi-periodic boundary conditions

$$e_k|_{\Sigma_R} = e^{ik|a_1|} e_k|_{\Sigma_L}, \quad \partial_{\mathbf{n}} e_k|_{\Sigma_R} = -e^{ik|a_1|} \partial_{\mathbf{n}} e_k|_{\Sigma_L}, \quad (2.1b)$$

at the left  $\Sigma_L = \Sigma_L^+ \cup \Sigma_L^0 \cup \Sigma_L^- \subset \partial S$  and right  $\Sigma_R = \Sigma_R^+ \cup \Sigma_R^0 \cup \Sigma_R^- \subset \partial S$  boundaries of  $S$ , and a decay condition for  $|x_2| \rightarrow \infty$ . The parameter  $k \in B$  is the so-called quasi-momentum in the one-dimensional Brillouin zone  $B = [-\pi/|a_1|, \pi/|a_1|]$ , and the operator  $\partial_{\mathbf{n}}$  denotes the normal derivative, *i. e.*  $\partial_{\mathbf{n}} = \mathbf{n} \cdot \nabla$  with the unit normal vector  $\mathbf{n}$  outward to the domain  $S$ .

## 2.3 Model problem of finding surface modes

The computation of surface modes is the second model problem that we want to introduce. In comparison to guided modes, surface modes are modes that are guided along the surface rather than a line defect. The computational domain of the surface mode problem is in principle equivalent to the one of the guided mode problem sketched in Figure 2.1, except that the top (or bottom) half plane  $\Omega^+$  (or  $\Omega^-$ ) are replaced by a medium for which the electric field  $E$  (TM-mode) or the magnetic field  $H$  (TE-mode) vanishes, and the permittivity  $\varepsilon_{\text{defect}}$  in the line defect is chosen to be equivalent to the permittivity  $\varepsilon_{\text{PhC}}^-$  (or  $\varepsilon_{\text{PhC}}^+$ ). Taking the line defect  $\Omega_{\text{defect}}$  into account, guarantees that we can simply use all results of this paper that are developed for the guided mode problem. In other words, the surface modes are defined as the non trivial solutions of

$$-\Delta e_k(\mathbf{x}) - \omega^2 \varepsilon(\mathbf{x}) e_k(\mathbf{x}) = 0 \quad (2.2a)$$

in the half-infinite strip  $C_0 \cup S^- \subset \mathbb{R}^2$  which satisfy quasi-periodic boundary conditions

$$e_k|_{\Sigma_R} = e^{ik|a_1|}e_k|_{\Sigma_L}, \quad \partial_{\mathbf{n}}e_k|_{\Sigma_R} = -e^{ik|a_1|}\partial_{\mathbf{n}}e_k|_{\Sigma_L}, \quad (2.2b)$$

at the left and right boundaries  $\Sigma_L$  and  $\Sigma_R$ , respectively, a homogeneous Dirichlet boundary condition

$$e_k|_{\Gamma_0^+} = 0, \quad (2.2c)$$

at the top boundary  $\Gamma_0^+ = \overline{C_0} \cap \overline{C_1^+}$ , and a decay condition for  $x_2 \rightarrow -\infty$ .

#### 2.4 Transformation to periodic problem and spectral properties

In this section we will briefly summarize some spectral properties of problem (2.1). For more details and proofs the reader is referred to [5] and [13].

Before we can present the spectral properties we need to introduce several function spaces. Let  $H^1(S)$  be the usual space of square integrable functions in  $S$  whose gradient is also square integrable. Then we define the periodic space

$$H_{\text{per}}^1(S) := \left\{ u \in H^1(S) \text{ with } u|_{\Sigma_L} = u|_{\Sigma_R} \right\}.$$

Moreover, let  $H^1(\Delta, S)$  be the subspace of  $H^1(S)$  with functions whose Laplacian is square integrable. Then we define

$$H_{\text{per}}^1(\Delta, S) := \left\{ u \in H^1(\Delta, S) \cap H_{\text{per}}^1(S) \text{ with } \partial_{\mathbf{n}}u|_{\Sigma_L} = -\partial_{\mathbf{n}}u|_{\Sigma_R} \right\}.$$

Let  $\Gamma_0^\pm = \partial S^\pm \cap \partial C_0$  denote the boundaries between the top and bottom half-strips  $S^\pm$  and the defect cell  $C_0$ . Then we define  $H_{\text{per}}^{1/2}(\Gamma_0^\pm)$  as the trace of  $H_{\text{per}}^1(S^\pm)$  on the boundary  $\Gamma_0^\pm$  and  $H_{\text{per}}^{-1/2}(\Gamma_0^\pm)$  as its dual space.

With these definitions and the substitution  $e_k(\mathbf{x}) = e^{ikx_1}u(\mathbf{x})$ , the eigenvalue problem (2.1) is equivalent to: find  $(\omega^2, k) \in \mathbb{R}^+ \times B$  such that there exists a non-trivial  $u \in H_{\text{per}}^1(\Delta, S)$  that satisfies

$$-(\nabla + ik\mathbf{a}_1) \cdot (\nabla + ik\mathbf{a}_1)u(\mathbf{x}) - \omega^2\varepsilon(\mathbf{x})u(\mathbf{x}) = 0, \quad \mathbf{x} \in S. \quad (2.3)$$

Then we call  $(\omega^2, k)$  an *eigenvalue couple* of (2.3) with associated eigenfunction  $u$ . This eigenvalue problem is linear in  $\omega^2$  when fixing  $k \in B$ , the so called  *$\omega$ -formulation*, and quadratic in  $k$  when fixing  $\omega \in \mathbb{R}^+$ , the so called  *$k$ -formulation*. However, note that this problem is posed on the unbounded domain  $S$ .

Now let us come to the spectral properties of (2.3) as shown in [5, 13], which are relevant for this work. For any  $k \in B$  we will denote the set of frequencies  $\omega^2$  for which Bloch modes [14] in the PhC  $\Omega_{\text{PhC}}^+$  on top or in the PhC  $\Omega_{\text{PhC}}^-$  below the defect exist by  $\sigma_{\text{ess}}(k) \subset \mathbb{R}^+$ . This set, called *essential spectrum* of the operator related to the eigenvalue problem (2.3), satisfies

$$\sigma_{\text{ess}}(k) = \mathbb{R}^+ \setminus \bigcup_{n=1}^{N(k)} I_n(k),$$

with  $N(k)$  open intervals  $I_n(k) \subset \mathbb{R}^+$ , the so called *band gaps* [13] ( $0 \leq N(k) \leq \infty$ ). We suppose in the following that there exists at least one band gap ( $N(k) \geq 1$ ). Inside the band gaps  $I_n(k)$ ,  $n = 1, \dots, N(k)$ ,  $k \in B$ , there exist only isolated eigenvalues of finite multiplicity which can only accumulate at the boundaries of the band gaps  $I_n(k)$  [5]. Let the isolated eigenvalues  $\omega_m^2(k)$ ,  $m = 1, \dots, M(k)$ , of (2.3) inside the band gaps  $I_n(k)$ ,  $n = 1, \dots, N(k)$ , be ordered such that

$$0 \leq \omega_1^2(k) \leq \dots \leq \omega_{M(k)}^2(k)$$

with  $0 \leq M(k) \leq \infty$ . Then we can define so called *dispersive curves* (of the first kind)

$$f_m^{(1)}(k) = \omega_m^2(k), \quad m = 1, \dots, M(k),$$

that are  $\frac{2\pi}{|a_1|}$ -periodic, even and continuous [5]. On the other hand, there exists an alternative ordering  $m \mapsto \tilde{m}(m)$  of the eigenvalues  $\omega_m^2(k)$ ,  $m = 1, \dots, M(k)$ , such that the dispersive curves of the second kind

$$f_m^{(2)}(k) = \omega_{\tilde{m}(m)}^2(k), \quad m = 1, \dots, M(k),$$

are analytic [12].

### 3 The Robin-to-Robin operators

In this section we define the RtR operators, show their characterization using local cell problems and a quadratic operator equation. Finally, we will elaborate on the discretization of the RtR operators and the local cell problems.

#### 3.1 Definition of the Robin-to-Robin operators

The RtR operators are defined through Robin problems in the infinite half-strips  $S^\pm$ . But before we introduce these problems, let us give some introductory remarks on the RtR operators and all other (local) operators that we will introduce later in this section and that map a Robin trace to another Robin trace. We will classify Robin traces in this work by *forward* and *backward*. Note that any Robin trace can be split into a Neumann trace (with a certain direction) and a Dirichlet trace. We will denote a Robin trace as forward, if its Neumann trace points away from the line defect, and, on the other hand, the Robin trace is called backward, if its Neumann trace points towards the line defect. For example, let  $v \in H_{\text{per}}^1(\Delta, S)$ , then  $\partial_2 v$  is a forward Robin trace in the infinite half-strip  $S^+$  whereas it is a backward Robin trace in  $S^-$ . While the directions of the Neumann traces vary in this work (either forward or backward), the Dirichlet traces are always the same. The Robin traces that we will deal with in this work always take the form  $\pm \partial_2 v + i\alpha v$  with some  $\alpha \in \mathbb{R} \setminus \{0\}$ .

Now let us come to the Robin problems in the infinite half-strips  $S^\pm$ . For any forward Robin trace  $\varphi \in H_{\text{per}}^{-1/2}(\Gamma_0^\pm)$  we seek  $u^\pm(\varphi) \equiv u^\pm(\cdot; \omega, k, \varphi) \in H_{\text{per}}^1(\Delta, S^\pm)$  such that

$$-(\nabla + i\mathbf{k}\mathbf{a}_1) \cdot (\nabla + i\mathbf{k}\mathbf{a}_1)u^\pm(\varphi) - \omega^2 \varepsilon u^\pm(\varphi) = 0 \quad \text{in } S^\pm, \quad (3.1a)$$

$$(\pm\partial_2 + i\alpha)u^\pm(\varphi) = \varphi \quad \text{on } \Gamma_0^\pm. \quad (3.1b)$$

The following result is the main advantage of the RtR method compared to the DtN method [4].

**Theorem 3.1** *If  $\omega^2 \notin \sigma_{\text{ess}}^\pm(k)$ , the problem (3.1) is well-posed in  $H_{\text{per}}^1(\Delta, S^\pm)$ .*

Theorem 3.1 guarantees well-posedness of (3.1) at all frequencies  $\omega^2 \notin \sigma_{\text{ess}}^\pm(k)$ . If the Robin boundary condition is replaced by a Dirichlet boundary condition, as done in [5, 13] for the DtN method, the problem is well posed except for a countable set of frequencies  $\omega^2$  which corresponds to the Dirichlet eigenvalues of the problem in the infinite half-strip. We will call these frequencies *global Dirichlet eigenvalues*.

Then, for any forward Robin trace  $\varphi \in H_{\text{per}}^{-1/2}(\Gamma_0^\pm)$  on  $\Gamma_0^\pm$ , the RtR operators  $\mathcal{R}^\pm(\omega, k) \in \mathcal{L}(H_{\text{per}}^{-1/2}(\Gamma_0^\pm))$  are defined as the backward Robin trace of  $u^\pm(\cdot; \omega, k, \varphi)$  on  $\Gamma_0^\pm$ , *i. e.*

$$\mathcal{R}^\pm(\omega, k)\varphi = (\mp\partial_2 + i\alpha)u^\pm(\cdot; \omega, k, \varphi)|_{\Gamma_0^\pm}. \quad (3.2)$$

### 3.2 Characterization of the Robin-to-Robin operators

In this subsection we explain how we can compute the RtR operators using local cell problems and a quadratic operator equation.

First, we note that the infinite strips  $S^\pm$  on top and bottom of the guide can be expressed as union of an infinite number of periodicity cells  $C_n^\pm$ ,  $n \in \mathbb{N}$ , *i. e.*  $S^\pm = \bigcup_{n=1}^\infty C_n^\pm$ , *c. f.* Figure 2.1(b). The top and bottom boundaries of these cells  $C_n^\pm$  shall be denoted by  $\Gamma_{n-1}^\pm$  and  $\Gamma_n^\pm$ , *i. e.*  $\Gamma_0^\pm = \overline{C_0} \cap \overline{C_1}^\pm$  and  $\Gamma_n^\pm = \overline{C_n} \cap \overline{C_{n+1}}^\pm$  for  $n \geq 1$ . We also note that — due to the periodicity and the infinity of the half strips — all cells  $C_n^\pm$  can be identified by the first cell  $C_1^\pm$  and all boundaries  $\Gamma_n^\pm$  can be identified by the first boundary  $\Gamma_0^\pm$ . This implies that we can identify all functions of  $C_n^\pm$  by functions of  $C_1^\pm$ , and, similarly, all functions of  $\Gamma_n^\pm$  by functions of  $\Gamma_0^\pm$ . In [13] we introduced shift operators that allow for a rigorous notation of this identification. However, for simplicity of notation we shall refrain from introducing these shift operators in this work, keeping in mind, that such an identification is possible.

We start by introducing two propagation operators.

- The forward-forward propagation operator  $\mathcal{P}_{\text{ff}}^\pm(\omega, k) \in \mathcal{L}(H_{\text{per}}^{-1/2}(\Gamma_0^\pm))$ , defined by

$$\mathcal{P}_{\text{ff}}^\pm(\omega, k)\varphi = (\pm\partial_2 + i\alpha)u^\pm(\cdot; \omega, k, \varphi)|_{\Gamma_1^\pm},$$

maps the forward Robin trace  $\varphi \in H_{\text{per}}^{-1/2}(\Gamma_0^\pm)$  on  $\Gamma_0^\pm$  to the forward Robin trace of the infinite half-strip solution  $u^\pm(\varphi)$  of (3.1) on  $\Gamma_1^\pm$ . This operator is compact (using interior elliptic regularity of the solution), injective (using the well



posedness of problem (3.1) and unique continuation arguments), and its spectral radius is strictly less than one (this is linked to the  $L^2$ -property of the solution  $u^\pm(\cdot; \omega, k, \varphi)$ ). The proof of these properties is the same as in [11, 4].

- The forward-backward propagation operator  $\mathcal{P}_{\text{fb}}^\pm(\omega, k) \in \mathcal{L}(H_{\text{per}}^{-1/2}(\Gamma_0^\pm))$ , defined by

$$\mathcal{P}_{\text{fb}}^\pm(\omega, k)\varphi = (\mp\partial_2 + i\alpha)u^\pm(\cdot; \omega, k, \varphi)|_{\Gamma_1^\pm},$$

maps the forward Robin trace  $\varphi \in H_{\text{per}}^{-1/2}(\Gamma_0^\pm)$  on  $\Gamma_0^\pm$  to the backward Robin trace of the infinite half-strip solution  $u^\pm(\varphi)$  on  $\Gamma_1^\pm$ .

Now we define local cell problems: for any forward Robin trace  $\varphi \in H_{\text{per}}^{-1/2}(\Gamma_0^\pm)$  on  $\Gamma_0^\pm$  and any backward Robin trace  $\psi \in H_{\text{per}}^{-1/2}(\Gamma_1^\pm)$  on  $\Gamma_1^\pm$  find  $u_{\text{loc}}^\pm(\varphi, \psi) \equiv u_{\text{loc}}^\pm(\cdot; \omega, k, \varphi, \psi) \in H_{\text{per}}^1(\Delta, C_1^\pm)$  as solution of

$$-(\nabla + ika_1) \cdot (\nabla + ika_1)u_{\text{loc}}^\pm(\varphi, \psi) - \omega^2 \varepsilon u_{\text{loc}}^\pm(\varphi, \psi) = 0 \quad \text{in } C_1^\pm, \quad (3.3a)$$

$$(\pm\partial_2 + i\alpha)u_{\text{loc}}^\pm(\varphi, \psi) = \varphi \quad \text{on } \Gamma_0^\pm, \quad (3.3b)$$

$$(\mp\partial_2 + i\alpha)u_{\text{loc}}^\pm(\varphi, \psi) = \psi \quad \text{on } \Gamma_1^\pm. \quad (3.3c)$$

These local cell problems are well-posed for all  $(\omega^2, k) \in \mathbb{R}^+ \times B$ . The corresponding Dirichlet cell problems, however, that are used in [5, 13] to characterize the DtN operators, are only well-posed if we exclude for each  $k \in B$  a countable set of frequencies  $\omega^2$  — the eigenvalues of the local cell problem (3.3a) with homogeneous Dirichlet boundary conditions at  $\Gamma_0^\pm$  and  $\Gamma_1^\pm$ . We will call these frequencies *local Dirichlet eigenvalues*.

With the solutions of the local cell problems (3.3) we define the local RtR operators

$$\mathcal{T}_{\text{fb}}^\pm(\omega, k)\varphi = (\mp\partial_2 + i\alpha)u_{\text{loc}}^\pm(\varphi, 0)|_{\Gamma_0^\pm}, \quad (3.4a)$$

which maps the forward Robin trace  $\varphi$  on  $\Gamma_0^\pm$  to the backward Robin trace of the local cell solution  $u_{\text{loc}}^\pm(\varphi, 0)$  on  $\Gamma_0^\pm$ ,

$$\mathcal{T}_{\text{ff}}^\pm(\omega, k)\varphi = (\pm\partial_2 + i\alpha)u_{\text{loc}}^\pm(\varphi, 0)|_{\Gamma_1^\pm}, \quad (3.4b)$$

which maps the forward Robin trace  $\varphi$  on  $\Gamma_0^\pm$  to the forward Robin trace of the local cell solution  $u_{\text{loc}}^\pm(\varphi, 0)$  on  $\Gamma_1^\pm$ ,

$$\mathcal{T}_{\text{bb}}^\pm(\omega, k)\psi = (\mp\partial_2 + i\alpha)u_{\text{loc}}^\pm(0, \psi)|_{\Gamma_0^\pm}, \quad (3.4c)$$

which maps the backward Robin trace  $\psi$  on  $\Gamma_1^\pm$  to the backward Robin trace of the local cell solution  $u_{\text{loc}}^\pm(0, \psi)$  on  $\Gamma_0^\pm$ , and

$$\mathcal{T}_{\text{bf}}^\pm(\omega, k)\psi = (\pm\partial_2 + i\alpha)u_{\text{loc}}^\pm(0, \psi)|_{\Gamma_1^\pm}, \quad (3.4d)$$

which maps the backward Robin trace  $\psi$  on  $\Gamma_1^\pm$  to the forward Robin trace of the local cell solution  $u_{\text{loc}}^\pm(0, \psi)$  on  $\Gamma_1^\pm$ .

With the help of the local cell solutions and the propagation operators  $\mathcal{P}_{\text{ff}}^\pm$  and  $\mathcal{P}_{\text{fb}}^\pm$  we can express the infinite half strip solution  $u^\pm(\varphi)$  in the cell  $C_n^\pm$ ,  $n \in \mathbb{N}$ , as

$$\begin{aligned} u^\pm(\varphi)|_{C_n^\pm} &= u_{\text{loc}}^\pm((\mathcal{P}_{\text{ff}}^\pm)^{n-1}\varphi, \mathcal{P}_{\text{fb}}^\pm(\mathcal{P}_{\text{ff}}^\pm)^{n-1}\varphi) \\ &= u_{\text{loc}}^\pm((\mathcal{P}_{\text{ff}}^\pm)^{n-1}\varphi, 0) + u_{\text{loc}}^\pm(0, \mathcal{P}_{\text{fb}}^\pm(\mathcal{P}_{\text{ff}}^\pm)^{n-1}\varphi), \end{aligned} \quad (3.5)$$

since the solutions of the local cell problems (3.3) are linear in the data  $(\varphi, \psi)$ . Evaluating the forward Robin trace of the infinite half-strip solution  $u^\pm(\varphi)$  on  $\Gamma_1^\pm$  using Eq. (3.5), we obtain an equation for the forward-forward propagation operator  $\mathcal{P}_{\text{ff}}^\pm$  in terms of the local RtR operators  $\mathcal{T}_{\text{ff}}^\pm$  and  $\mathcal{T}_{\text{bf}}^\pm$ , and the forward-backward propagation operator  $\mathcal{P}_{\text{fb}}^\pm$

$$\begin{aligned} \mathcal{P}_{\text{ff}}^\pm(\omega, k)\varphi &= [(\pm\partial_2 + i\alpha)u^\pm(\varphi)]|_{\Gamma_1^\pm} \\ &= [(\pm\partial_2 + i\alpha)u_{\text{loc}}^\pm(\varphi, 0)]|_{\Gamma_1^\pm} + [(\pm\partial_2 + i\alpha)u_{\text{loc}}^\pm(0, \mathcal{P}_{\text{fb}}^\pm\varphi)]|_{\Gamma_1^\pm} \\ &= \mathcal{T}_{\text{ff}}^\pm\varphi + \mathcal{T}_{\text{bf}}^\pm\mathcal{P}_{\text{fb}}^\pm\varphi. \end{aligned} \quad (3.6)$$

On the other hand, identifying the backward Robin trace of the infinite half-strip solution  $u^\pm(\varphi)$  on  $\Gamma_1^\pm$  by the backward Robin trace of the infinite half-strip solution  $u^\pm(\mathcal{P}_{\text{ff}}^\pm\varphi)$  on  $\Gamma_0^\pm$ , and evaluating this trace using Eq. (3.5), we obtain an equation for the forward-backward propagation operator  $\mathcal{P}_{\text{fb}}^\pm$  in terms of the local RtR operators  $\mathcal{T}_{\text{fb}}^\pm$  and  $\mathcal{T}_{\text{bb}}^\pm$ , and the forward-forward propagation operator  $\mathcal{P}_{\text{ff}}^\pm$

$$\begin{aligned} \mathcal{P}_{\text{fb}}^\pm(\omega, k)\varphi &= [(\mp\partial_2 + i\alpha)u^\pm(\varphi)]|_{\Gamma_1^\pm} \\ &= [(\mp\partial_2 + i\alpha)u^\pm(\mathcal{P}_{\text{ff}}^\pm\varphi)]|_{\Gamma_0^\pm} \\ &= [(\mp\partial_2 + i\alpha)u_{\text{loc}}^\pm(\mathcal{P}_{\text{ff}}^\pm\varphi, 0)]|_{\Gamma_0^\pm} + [(\mp\partial_2 + i\alpha)u_{\text{loc}}^\pm(0, \mathcal{P}_{\text{fb}}^\pm\mathcal{P}_{\text{ff}}^\pm\varphi)]|_{\Gamma_0^\pm} \\ &= \mathcal{T}_{\text{fb}}^\pm\mathcal{P}_{\text{ff}}^\pm\varphi + \mathcal{T}_{\text{bb}}^\pm\mathcal{P}_{\text{fb}}^\pm\mathcal{P}_{\text{ff}}^\pm\varphi. \end{aligned} \quad (3.7)$$

**Lemma 3.1** *The local RtR operator  $\mathcal{T}_{\text{bf}}^\pm(\omega, k)$  is invertible.*

*Proof* For any forward Robin trace  $\varphi \in H_{\text{per}}^{-1/2}(\Gamma_0^\pm)$  on  $\Gamma_0^\pm$  and any backward Robin trace  $\psi \in H_{\text{per}}^{-1/2}(\Gamma_1^\pm)$  on  $\Gamma_1^\pm$ , let us introduce  $v^\pm(\varphi, \psi) \equiv v^\pm(\cdot; \omega, k, \varphi, \psi) \in H_{\text{per}}^1(\Delta, C_1^\pm)$  as the unique solution of

$$\begin{aligned} -(\nabla + i\mathbf{k}\mathbf{a}_1) \cdot (\nabla + i\mathbf{k}\mathbf{a}_1)v^\pm(\varphi, \psi) - \omega^2\varepsilon v^\pm(\varphi, \psi) &= 0 && \text{in } C_1^\pm, \\ (\pm\partial_2 + i\alpha)v^\pm(\varphi, \psi) &= \varphi && \text{on } \Gamma_0^\pm, \\ (\pm\partial_2 + i\alpha)v^\pm(\varphi, \psi) &= \psi && \text{on } \Gamma_1^\pm, \end{aligned}$$

and let  $\tilde{\mathcal{T}}_{\text{bf}}^\pm(\omega, k)$  be defined for all  $\psi \in H_{\text{per}}^{-1/2}(\Gamma_1^\pm)$  by

$$\tilde{\mathcal{T}}_{\text{bf}}^\pm(\omega, k)\psi = (\mp\partial_2 + i\alpha)v^\pm(0, \psi)|_{\Gamma_1^\pm}.$$

We can show easily that for all  $\psi \in H_{\text{per}}^{-1/2}(\Gamma_1^\pm)$

$$(\mp \partial_2 + i\alpha)v^\pm(0, \mathcal{T}_{\text{bf}}^\pm(\omega, k)\psi)|_{\Gamma_1^\pm} = \psi,$$

which implies by definition of  $\tilde{\mathcal{T}}_{\text{bf}}^\pm(\omega, k)$  that for all  $\psi \in H_{\text{per}}^{-1/2}(\Gamma_1^\pm)$

$$\tilde{\mathcal{T}}_{\text{bf}}^\pm(\omega, k)\mathcal{T}_{\text{bf}}^\pm(\omega, k)\psi = \psi.$$

We have also

$$(\pm \partial_2 + i\alpha)u_{\text{loc}}^\pm(0, \tilde{\mathcal{T}}_{\text{bf}}^\pm(\omega, k)\psi)|_{\Gamma_1^\pm} = \psi,$$

which implies by definition of  $\mathcal{T}_{\text{bf}}^\pm(\omega, k)$  that for all  $\psi \in H_{\text{per}}^{-1/2}(\Gamma_1^\pm)$

$$\mathcal{T}_{\text{bf}}^\pm(\omega, k)\tilde{\mathcal{T}}_{\text{bf}}^\pm(\omega, k)\psi = \psi.$$

□

Using Lemma 3.1 we can rewrite (3.6) in the form

$$\mathcal{P}_{\text{fb}}^\pm \varphi = (\mathcal{T}_{\text{bf}}^\pm)^{-1} (\mathcal{P}_{\text{ff}}^\pm \varphi - \mathcal{T}_{\text{ff}}^\pm \varphi). \quad (3.8)$$

Inserting this equality into Eq. (3.7) yields a quadratic operator equation, the so-called *Ricatti equation*,

$$\mathcal{T}_{\text{bb}}^\pm (\mathcal{T}_{\text{bf}}^\pm)^{-1} (\mathcal{P}_{\text{ff}}^\pm)^2 + \left( \mathcal{T}_{\text{fb}}^\pm - (\mathcal{T}_{\text{bf}}^\pm)^{-1} - \mathcal{T}_{\text{bb}}^\pm (\mathcal{T}_{\text{bf}}^\pm)^{-1} \mathcal{T}_{\text{ff}}^\pm \right) \mathcal{P}_{\text{ff}}^\pm + (\mathcal{T}_{\text{bf}}^\pm)^{-1} \mathcal{T}_{\text{ff}}^\pm = 0. \quad (3.9)$$

**Proposition 3.1** *Let  $\omega^2 \notin \sigma_{\text{ess}}^\pm(k)$ . Then the forward-forward propagation operator  $\mathcal{P}_{\text{ff}}^\pm(\omega, k)$  is the unique solution of the Ricatti equation (3.9) with spectral radius  $\rho(\mathcal{P}_{\text{ff}}^\pm) < 1$ .*

*Proof* We showed already that  $\mathcal{P}_{\text{ff}}^\pm(\omega, k)$  is solution of the Ricatti equation (3.9). To show that it is the unique solution, we use the same ideas as in [11, 4] and suppose that  $\tilde{\mathcal{P}}_{\text{ff}}^\pm$  is also a solution. Let us introduce

$$\tilde{\mathcal{P}}_{\text{fb}}^\pm = (\mathcal{T}_{\text{bf}}^\pm)^{-1} (\tilde{\mathcal{P}}_{\text{ff}}^\pm - \mathcal{T}_{\text{ff}}^\pm)$$

and define for all  $\varphi \in H_{\text{per}}^{-1/2}(\Gamma_0^\pm)$

$$v^\pm(\varphi)|_{C_n^\pm} = v^\pm((\tilde{\mathcal{P}}_{\text{ff}}^\pm)^{n-1} \varphi, \tilde{\mathcal{P}}_{\text{fb}}^\pm (\tilde{\mathcal{P}}_{\text{ff}}^\pm)^{n-1} \varphi).$$

We can see easily that  $v^\pm(\varphi)$  satisfies the boundary condition (3.1b) and is solution of (3.1a) in each cell  $C_n^\pm$ . We can also show the continuity of the forward and the backward traces on each  $\Gamma_n^\pm$  because  $\tilde{\mathcal{P}}_{\text{ff}}^\pm$  is solution of (3.9) and by definition of  $\tilde{\mathcal{P}}_{\text{fb}}^\pm$ . Finally,  $v^\pm(\varphi)$  is  $L^2(S^\pm)$  because the spectral radius of  $\tilde{\mathcal{P}}_{\text{ff}}^\pm$  is strictly less than one. Due to well-posedness of (3.1),  $v^\pm(\varphi)$  is necessarily equal to  $u_{\text{loc}}^\pm(\varphi)$  for each  $\varphi$  and in particular their traces on  $\Gamma_1^\pm$  coincide. Hence, the operator  $\tilde{\mathcal{P}}_{\text{ff}}^\pm$  is nothing else but  $\mathcal{P}_{\text{ff}}^\pm$ . □

Now let us come to an important result on the relation of the proposed RtR approach and the DtN approach as presented in [5]. To this end, we introduce the Dirichlet problems on the infinite half-strip: for any Dirichlet trace  $\varphi_{\text{DtN}} \in H_{\text{per}}^{1/2}(\Gamma_0^\pm)$  find  $u_{\text{DtN}}^\pm(\varphi_{\text{DtN}}) \equiv u_{\text{DtN}}^\pm(\cdot; \omega, k, \varphi_{\text{DtN}}) \in H_{\text{per}}^1(\Delta, S^\pm)$  that satisfies Eq. (3.1a) together with the Dirichlet boundary condition

$$u^\pm(\varphi_{\text{DtN}})|_{\Gamma_0^\pm} = \varphi_{\text{DtN}}. \quad (3.10)$$

Recall that this Dirichlet problem is only well-posed for  $(\omega^2, k) \in \mathbb{R}^+ \times B$  with  $\omega^2 \notin \sigma_{\text{ess}}(k)$  except a countable set of frequencies — the global Dirichlet eigenvalues, *i. e.* eigenvalues of (3.1a) with homogeneous Dirichlet boundary condition (3.10). Furthermore, let  $\mathcal{P}_{\text{DtN}}^\pm(\omega, k) \in \mathcal{L}(H_{\text{per}}^{1/2}(\Gamma_0^\pm))$  denote the Dirichlet-to-Dirichlet propagation operator of the DtN approach, *i. e.* for  $\varphi_{\text{DtN}} \in H_{\text{per}}^{1/2}(\Gamma_0^\pm)$  we define  $\mathcal{P}_{\text{DtN}}^\pm \varphi_{\text{DtN}} = u_{\text{DtN}}^\pm(\varphi_{\text{DtN}})|_{\Gamma_1^\pm}$ . Then we can show the following result.

**Proposition 3.2** *Let  $(\omega^2, k) \in \mathbb{R}^+ \times B$  with  $\omega^2 \notin \sigma_{\text{ess}}(k)$  and let the infinite half-strip problem (3.1a) with Dirichlet condition (3.10) be well-posed. Then the following holds true: If  $\mu_{\text{DtN}}^\pm \in \mathbb{C}$  is an eigenvalue of  $\mathcal{P}_{\text{DtN}}^\pm(\omega, k)$  with associated eigenfunction  $\varphi_{\text{DtN}}^\pm \in H_{\text{per}}^{1/2}(\Gamma_0^\pm)$ , *i. e.*  $\mathcal{P}_{\text{DtN}}^\pm(\omega, k)\varphi_{\text{DtN}}^\pm = \mu_{\text{DtN}}^\pm \varphi_{\text{DtN}}^\pm$ , then  $\mu_{\text{DtN}}^\pm$  is also an eigenvalue of the forward-forward RtR propagation operator  $\mathcal{P}_{\text{ff}}^\pm(\omega, k)$  with associated eigenfunction*

$$\varphi^\pm = \pm \partial_2 u_{\text{DtN}}^\pm(\varphi_{\text{DtN}}^\pm) + i\alpha \varphi_{\text{DtN}}^\pm \in H_{\text{per}}^{-1/2}(\Gamma_0^\pm).$$

*Proof* Let  $\mu_{\text{DtN}}^\pm \in \mathbb{C}$  be an eigenvalue of  $\mathcal{P}_{\text{DtN}}^\pm(\omega, k)$  with associated eigenfunction  $\varphi_{\text{DtN}}^\pm \in H_{\text{per}}^{1/2}(\Gamma_0^\pm)$ . Then  $u_{\text{DtN}}^\pm(\varphi_{\text{DtN}}^\pm)$  solves the Robin problem (3.1) with  $\varphi = \varphi_{\text{RtR}}^\pm := \pm \partial_2 u_{\text{DtN}}^\pm(\varphi_{\text{DtN}}^\pm) + i\alpha \varphi_{\text{DtN}}^\pm$ . But this implies that  $u^\pm(\varphi_{\text{RtR}}^\pm) \equiv u_{\text{DtN}}^\pm(\varphi_{\text{DtN}}^\pm)$  and hence,

$$\begin{aligned} \mathcal{P}_{\text{ff}}^\pm(\omega, k)\varphi_{\text{RtR}}^\pm &= (\pm \partial_2 + i\alpha)u_{\text{DtN}}^\pm(\varphi_{\text{RtR}}^\pm)|_{\Gamma_1^\pm} \\ &= \mu_{\text{DtN}}^\pm(\pm \partial_2 + i\alpha)u_{\text{DtN}}^\pm(\varphi_{\text{RtR}}^\pm)|_{\Gamma_0^\pm} \\ &= \mu_{\text{DtN}}^\pm \varphi_{\text{RtR}}^\pm, \end{aligned}$$

which finishes the proof.  $\square$

Once the forward-forward propagation operator  $\mathcal{P}_{\text{ff}}^\pm(\omega, k)$  is computed using the Ricatti equation (3.9) we can determine the forward-backward propagation operator  $\mathcal{P}_{\text{fb}}^\pm(\omega, k)$  from Eq. (3.8). The RtR operator  $\mathcal{R}^\pm(\omega, k)$  defined in (3.2), which maps a forward Robin trace on  $\Gamma_0^\pm$  to a backward Robin trace on  $\Gamma_0^\pm$ , can then be computed by

$$\begin{aligned} \mathcal{R}^\pm(\omega, k) &= \mathcal{T}_{\text{fb}}^\pm(\omega, k) + \mathcal{T}_{\text{bb}}^\pm(\omega, k)\mathcal{P}_{\text{fb}}^\pm(\omega, k) \\ &= \mathcal{T}_{\text{fb}}^\pm(\omega, k) + \mathcal{T}_{\text{bb}}^\pm(\omega, k)(\mathcal{T}_{\text{bf}}^\pm(\omega, k))^{-1}\mathcal{P}_{\text{ff}}^\pm(\omega, k) \\ &\quad - \mathcal{T}_{\text{bb}}^\pm(\omega, k)(\mathcal{T}_{\text{bf}}^\pm(\omega, k))^{-1}\mathcal{T}_{\text{ff}}^\pm(\omega, k). \end{aligned} \quad (3.11)$$

### 3.3 Variational formulation of the local cell problems

The derivation of the weak formulation of the local cell problem (3.3) is easy. Using standard techniques, we can deduce that Eq. (3.3) is equivalent to: for given forward Robin trace  $\varphi$  on  $\Gamma_0^\pm$  and backward Robin trace  $\psi$  on  $\Gamma_1^\pm$  find  $u_{\text{loc}}^\pm(\varphi, \psi) \in H_{\text{per}}^1(C_1^\pm)$  such that

$$\begin{aligned} \int_{C_1^\pm} (\nabla + i\mathbf{k}\mathbf{a}_1)u_{\text{loc}}^\pm(\varphi, \psi) \cdot (\nabla - i\mathbf{k}\mathbf{a}_1)\bar{v} - \omega^2 \varepsilon u_{\text{loc}}^\pm(\varphi, \psi)\bar{v} \, d\mathbf{x} \\ - i\alpha \sum_{j=0,1} \int_{\Gamma_j^\pm} u_{\text{loc}}^\pm(\varphi, \psi) \bar{v} \, ds(\mathbf{x}) = - \int_{\Gamma_0^\pm} \varphi \bar{v} \, ds(\mathbf{x}) - \int_{\Gamma_1^\pm} \psi \bar{v} \, ds(\mathbf{x}) \end{aligned} \quad (3.12)$$

for all  $v \in H_{\text{per}}^1(C_1^\pm)$ , where we rewrote the boundary conditions (3.3b) and (3.3c) in the form

$$\mp \partial_2 u_{\text{loc}}^\pm(\varphi, \psi) = i\alpha u_{\text{loc}}^\pm(\varphi, \psi) - \varphi \quad \text{on } \Gamma_0^\pm, \quad (3.13a)$$

$$\pm \partial_2 u_{\text{loc}}^\pm(\varphi, \psi) = i\alpha u_{\text{loc}}^\pm(\varphi, \psi) - \psi \quad \text{on } \Gamma_1^\pm, \quad (3.13b)$$

to replace the Neumann trace that appears when using integration by parts.

Once the local cell solutions  $u_{\text{loc}}^\pm(\varphi, \psi)$  are known, we can compute the local RtR operators by inserting (3.13) into the definition (3.4) of the local RtR operators which yields

$$\mathcal{J}_{\text{fb}}^\pm(\omega, k)\varphi = 2i\alpha u_{\text{loc}}^\pm(\varphi, 0)|_{\Gamma_0^\pm} - \varphi, \quad (3.14a)$$

$$\mathcal{J}_{\text{ff}}^\pm(\omega, k)\varphi = 2i\alpha u_{\text{loc}}^\pm(\varphi, 0)|_{\Gamma_1^\pm}, \quad (3.14b)$$

$$\mathcal{J}_{\text{bb}}^\pm(\omega, k)\psi = 2i\alpha u_{\text{loc}}^\pm(0, \psi)|_{\Gamma_0^\pm}, \quad (3.14c)$$

$$\mathcal{J}_{\text{bf}}^\pm(\omega, k)\psi = 2i\alpha u_{\text{loc}}^\pm(0, \psi)|_{\Gamma_1^\pm} - \psi. \quad (3.14d)$$

### 3.4 Discretization

In Section 3.3 we introduced a variational formulation for the local cell problems to compute the local RtR operators (3.4). In this section we now want to introduce a finite element discretization of the spaces involved, and describe the computation of the discrete RtR maps. Most parts — including the choice of the meshes, the finite element spaces, and the refinement strategies — can directly be recalled from the discretization of the DtN maps in [13]. Therefore, we shall only point out the most important issues and elaborate on some extensions specific to the RtR case while referring to [13] for more details.

Let  $\mathcal{M}_h(C_1^\pm)$  and  $\mathcal{M}_h(\Gamma_0^\pm)$  be the meshes of the computational domains  $C_1^\pm$  and  $\Gamma_0^\pm$ , respectively, with maximum mesh width  $h$ . Based on these meshes, let  $S_{\text{per}}^{p,1}(C_1^\pm)$  and  $S_{\text{per}}^{p,1}(\Gamma_0^\pm)$  denote the finite element subspaces of  $H_{\text{per}}^1(C_1^\pm)$  and  $H_{\text{per}}^{1/2}(\Gamma_0^\pm)$ , respectively, with polynomial degree  $p$  and dimensions  $N(C_1^\pm) = \dim S_{\text{per}}^{p,1}(C_1^\pm)$  and

1  $N(\Gamma_0^\pm) = \dim(\Gamma_0^\pm)$ . For the discretization of the local cell problems (3.12), we ad-  
 2 ditionally need a finite element subspace of the space  $H_{\text{per}}^{-1/2}(\Gamma_0^\pm)$  of the Neumann  
 3 and Robin traces. We shall assume in this work, that the boundaries  $\Gamma_0^\pm$  satisfy an  
 4 additional smoothness condition, *i. e.* there is no jump of the material coefficient  $\varepsilon(\mathbf{x})$   
 5 on  $\Gamma_0^\pm$ , and hence, we can expect higher regularity of the Neumann and Robin traces  
 6 such that we can simply choose  $S_{\text{per}}^{p,1}(\Gamma_0^\pm)$  as finite element subspace of  $H_{\text{per}}^{-1/2}(\Gamma_0^\pm)$ .  
 7 If, however, this additional smoothness condition of the boundaries is not fulfilled,  
 8 we need to introduce a finite element space for the Neumann and Robin traces that  
 9 can cope for their jump at the material interface. The space of piecewise discontinu-  
 10 ous polynomials may be an appropriate choice, but it has to be noted that the duality  
 11 product of this space with  $S_{\text{per}}^{p,1}(\Gamma_0^\pm)$  is not always of full rank. Using shifted meshes  
 12 as shown in [18] may resolve this problem. An alternative choice for the discrete sub-  
 13 space of  $H_{\text{per}}^{-1/2}(\Gamma_0^\pm)$  is defined by the biorthogonal basis proposed by Wohlmuth [20]  
 14 for mortar finite elements.

15 Again recall that all boundaries  $\Gamma_n^\pm$ ,  $n \in \mathbb{N}$ , can be identified with the first bound-  
 16 ary  $\Gamma_0^\pm$ . This implies — using appropriate finite element meshes — that  $S_{\text{per}}^{p,1}(\Gamma_0^\pm)$  is  
 17 also a subspace of  $H_{\text{per}}^{1/2}(\Gamma_1^\pm)$  and  $H_{\text{per}}^{-1/2}(\Gamma_1^\pm)$ .

### 18 3.4.1 Discretization of the local cell problems

19 In this subsection we aim to compute the discrete versions of the local RtR operators  
 20  $\mathcal{T}_{\text{fb}}^\pm$ ,  $\mathcal{T}_{\text{ff}}^\pm$ ,  $\mathcal{T}_{\text{bb}}^\pm$  and  $\mathcal{T}_{\text{bf}}^\pm$  in order to access the discrete forward-forward propagation  
 21 operators and discrete RtR operators in the following subsections.

22 Using the finite element spaces  $S_{\text{per}}^{p,1}(C_1^\pm)$  and  $S_{\text{per}}^{p,1}(\Gamma_0^\pm)$  we derive a discrete form  
 23 of the local cell problems (3.3): for given forward Robin trace  $\varphi_h \in S_{\text{per}}^{p,1}(\Gamma_0^\pm)$  on  $\Gamma_0^\pm$   
 24 and backward Robin trace  $\psi_h \in S_{\text{per}}^{p,1}(\Gamma_0^\pm)$  on  $\Gamma_1^\pm$  find  $u_{\text{loc,h}}^\pm(\varphi_h, \psi_h) \in S_{\text{per}}^{p,1}(C_1^\pm)$  such  
 25 that

$$\begin{aligned}
 & \int_{C_1^\pm} (\nabla + i k \mathbf{a}_1) u_{\text{loc,h}}^\pm(\varphi_h, \psi_h) \cdot (\nabla - i k \mathbf{a}_1) \bar{v}_h - \omega^2 \varepsilon u_{\text{loc,h}}^\pm(\varphi_h, \psi_h) \bar{v}_h \, d\mathbf{x} \\
 & - i \alpha \sum_{j=0,1} \int_{\Gamma_j^\pm} u_{\text{loc,h}}^\pm(\varphi_h, \psi_h) \bar{v}_h \, ds(\mathbf{x}) = - \int_{\Gamma_0^\pm} \varphi_h \bar{v}_h \, ds(\mathbf{x}) - \int_{\Gamma_1^\pm} \psi_h \bar{v}_h \, ds(\mathbf{x}) \quad (3.15)
 \end{aligned}$$

26 for all  $v_h \in S_{\text{per}}^{p,1}(C_1^\pm)$ , *c.f.* Eq. (3.12). These discrete local cell problems are well-  
 27 posed as long as the mesh width  $h$  is chosen small enough and the polynomial degree  
 28  $p$  is large enough [16, Thm. 4.2.9],[15].

29 The discrete local RtR operators are then defined as

$$30 \mathcal{T}_{\text{fb},h}^\pm(\omega, k) \varphi_h = 2i \alpha u_{\text{loc,h}}^\pm(\varphi_h, 0) |_{\Gamma_0^\pm} - \varphi_h, \quad (3.16a)$$

$$31 \mathcal{T}_{\text{ff},h}^\pm(\omega, k) \varphi_h = 2i \alpha u_{\text{loc,h}}^\pm(\varphi_h, 0) |_{\Gamma_1^\pm}, \quad (3.16b)$$

$$32 \mathcal{T}_{\text{bb},h}^\pm(\omega, k) \psi_h = 2i \alpha u_{\text{loc,h}}^\pm(0, \psi_h) |_{\Gamma_0^\pm}, \quad (3.16c)$$

$$33 \mathcal{T}_{\text{bf},h}^\pm(\omega, k) \psi_h = 2i \alpha u_{\text{loc,h}}^\pm(0, \psi_h) |_{\Gamma_1^\pm} - \psi_h, \quad (3.16d)$$

1  
2  
3  
4  
5  
6  
7  
8  
9  
10  
11  
12  
13  
14  
15  
16  
17  
18  
19  
20  
21  
22  
23  
24  
25  
26  
27  
28  
29  
30  
31  
32  
33  
34  
35  
36  
37  
38  
39  
40  
41  
42  
43  
44  
45  
46  
47  
48  
49  
50  
51  
52  
53  
54  
55  
56  
57  
58  
59  
60  
61  
62  
63  
64  
65

c.f. Eq. (3.14). Since the discrete local cell problems (3.15) are well-defined, it follows that the discrete local RtR operators (3.16) inherit their properties from the continuous local RtR operators (3.4). In particular,  $\mathcal{T}_{\text{bf},h}^{\pm}$  is invertible and hence,  $(\mathcal{T}_{\text{bf},h}^{\pm})^{-1}$  exists and is well-defined.

### 3.4.2 Linear system of equations for the local cell problems

Now we want to transform the discretized local cell problems (3.15) into linear systems of equations, and represent the discrete local RtR operators (3.16) in terms of matrices. First, we note that it is beneficial to order the basis functions  $b_{C_1^{\pm},n}$ ,  $n \in \mathcal{J}(C_1^{\pm}) = \{1, \dots, N(C_1^{\pm})\}$  of the finite element spaces  $S_{\text{per}}^{p,1}(C_1^{\pm})$  such that

- the basis functions of  $S_{\text{per}}^{p,1}(C_1^{\pm})$  with index  $n \in \mathcal{J}(C_1^{\pm}, \Gamma_0^{\pm}) = \{1, \dots, N(\Gamma_0^{\pm})\}$  vanish on  $\Gamma_1^{\pm}$  and build a basis of  $S_{\text{per}}^{p,1}(\Gamma_0^{\pm})$ ,
- the basis functions of  $S_{\text{per}}^{p,1}(C_1^{\pm})$  with index  $n \in \mathcal{J}(C_1^{\pm}, \Gamma_1^{\pm}) = \{N(\Gamma_0^{\pm}) + 1, \dots, 2N(\Gamma_0^{\pm})\}$  vanish on  $\Gamma_0^{\pm}$  and — if shifted to  $\Gamma_0^{\pm}$  — build a basis of  $S_{\text{per}}^{p,1}(\Gamma_0^{\pm})$ , and
- the basis functions of  $S_{\text{per}}^{p,1}(C_1^{\pm})$  with index  $n \in \mathcal{J}(C_1^{\pm}) \setminus (\mathcal{J}(C_1^{\pm}, \Gamma_0^{\pm}) \cup \mathcal{J}(C_1^{\pm}, \Gamma_1^{\pm})) = \{2N(\Gamma_0^{\pm}) + 1, \dots, N(C_1^{\pm})\}$  vanish on  $\Gamma_0^{\pm}$  and  $\Gamma_1^{\pm}$ .

With this special ordering we can introduce permutation matrices  $\mathbf{Q}_{C_1^{\pm}}^i \in \mathbb{R}^{N(\Gamma_0^{\pm}) \times N(\Gamma_0^{\pm})}$ ,  $i \in \{0, 1\}$ , such that

$$b_{\Gamma_0^{\pm},n} = \sum_{m=1}^{N(\Gamma_0^{\pm})} Q_{C_1^{\pm},mn}^0 b_{C_1^{\pm},m}|_{\Gamma_0^{\pm}} = \sum_{m=1}^{N(\Gamma_0^{\pm})} Q_{C_1^{\pm},mn}^1 b_{C_1^{\pm},N(\Gamma_0^{\pm})+m}|_{\Gamma_1^{\pm}}.$$

For simplicity of notation we shall assume in the following that the basis functions of  $S_{\text{per}}^{p,1}(C_1^{\pm})$  and  $S_{\text{per}}^{p,1}(\Gamma_0^{\pm})$  are ordered such that the permutation matrices are identity matrices of size  $N(\Gamma_0^{\pm}) \times N(\Gamma_0^{\pm})$ .

With the help of the basis  $b_{\Gamma_0^{\pm},n}$ ,  $n \in \{1, \dots, N(\Gamma_0^{\pm})\}$ , of the discrete space  $S_{\text{per}}^{p,1}(\Gamma_0^{\pm})$ , we seek matrix representations of the discrete local RtR operators  $\mathcal{T}_{ij,h}^{\pm}$ ,  $i, j \in \{\text{f}, \text{b}\}$ , i.e. we search for matrices  $\mathbf{T}_{ij}^{\pm} \in \mathbb{C}^{N(\Gamma_0^{\pm}) \times N(\Gamma_0^{\pm})}$  with coefficients  $T_{ij,mm}^{\pm}$ ,  $m, n \in \{1, \dots, N(\Gamma_0^{\pm})\}$  such that

$$\mathcal{T}_{ij,h}^{\pm} b_{\Gamma_0^{\pm},n} = \sum_{m=1}^{N(\Gamma_0^{\pm})} T_{ij,mm}^{\pm} b_{\Gamma_0^{\pm},m}, \quad i, j \in \{\text{f}, \text{b}\}. \quad (3.17)$$

Let  $\mathbf{A}_{C_1^{\pm}}(k) \in \mathbb{C}^{N(C_1^{\pm}) \times N(C_1^{\pm})}$  denote the matrix with coefficients

$$A_{C_1^{\pm},mm}(k) = \int_{C_1^{\pm}} (\nabla + ika_1) b_{C_1^{\pm},n} \cdot (\nabla - ika_1) \bar{b}_{C_1^{\pm},m} \, \mathbf{d}\mathbf{x},$$

$m, n \in \{1, \dots, N(C_1^{\pm})\}$ , c.f. Eq. (3.15). Similarly, let  $\mathbf{M}_{C_1^{\pm}}^{\varepsilon} \in \mathbb{R}^{N(C_1^{\pm}) \times N(C_1^{\pm})}$  denote the matrix with coefficients

$$M_{C_1^{\pm},mm}^{\varepsilon} = \int_{C_1^{\pm}} \varepsilon b_{C_1^{\pm},n} \bar{b}_{C_1^{\pm},m} \, \mathbf{d}\mathbf{x},$$

1  
2  
3  
4  
5  
6  
7  
8  
9  
10  
11  
12  
13  
14  
15  
16  
17  
18  
19  
20  
21  
22  
23  
24  
25  
26  
27  
28  
29  
30  
31  
32  
33  
34  
35  
36  
37  
38  
39  
40  
41  
42  
43  
44  
45  
46  
47  
48  
49  
50  
51  
52  
53  
54  
55  
56  
57  
58  
59  
60  
61  
62  
63  
64  
65

$m, n \in \{1, \dots, N(C_1^\pm)\}$ , *c.f.* Eq. (3.15). Moreover, let us introduce the matrices  $\mathbf{M}_{C_1^\pm}^{\Gamma_i^\pm} \in \mathbb{R}^{N(C_1^\pm) \times N(C_1^\pm)}$ ,  $i = 0, 1$ , with coefficients

$$M_{C_1^\pm, mn}^{\Gamma_i^\pm} = \int_{\Gamma_i^\pm} b_{C_1^\pm, n} \bar{b}_{C_1^\pm, m} \, ds(\mathbf{x}), \quad i = 0, 1,$$

$m, n \in \{1, \dots, N(C_1^\pm)\}$ , related to the boundary integrals in Eq. (3.15). With these matrices and the definition

$$\mathbf{S}_{C_1^\pm}^\varepsilon(\omega, k) := \mathbf{A}_{C_1^\pm}(k) - \omega^2 \mathbf{M}_{C_1^\pm}^\varepsilon - i\alpha \sum_{i=0,1} \mathbf{M}_{C_1^\pm}^{\Gamma_i^\pm},$$

the matrix form of the discrete local cell problem (3.12) reads

$$\mathbf{S}_{C_1^\pm}^\varepsilon(\omega, k) \mathbf{u}_{\text{loc},h}^\pm(b_{\Gamma_0^\pm, m}, b_{\Gamma_0^\pm, n}) = -\mathbf{M}_{C_1^\pm}^{\Gamma_0^\pm}(C_1^\pm, \Gamma_0^\pm) \mathbf{e}_m - \mathbf{M}_{C_1^\pm}^{\Gamma_1^\pm}(C_1^\pm, \Gamma_1^\pm) \mathbf{e}_n, \quad (3.18)$$

$m, n \in \{1, \dots, N(\Gamma_0^\pm)\}$ , where  $\mathbf{u}_{\text{loc},h}^\pm(b_{\Gamma_0^\pm, m}, b_{\Gamma_0^\pm, n}) \in \mathbb{C}^{N(C_1^\pm)}$  are the coefficient vectors of the discrete local cell solutions  $u_{\text{loc},h}(\cdot; \omega, k, b_{\Gamma_0^\pm, m}, b_{\Gamma_0^\pm, n}) \in S_{\text{per}}^{p,1}(C_1^\pm)$  with respect to the basis functions  $b_{C_1^\pm}$ ,  $\mathbf{M}_{C_1^\pm}^{\Gamma_i^\pm}(O_1, O_2)$  are the block matrices of  $\mathbf{M}_{C_1^\pm}^{\Gamma_i^\pm}$  with row indices  $\mathcal{J}(C_1^\pm, O_1)$  and column indices  $\mathcal{J}(C_1^\pm, O_2)$ , and  $\mathbf{e}_m, \mathbf{e}_n \in \mathbb{R}^{N(\Gamma_0^\pm)}$  are the  $m$ -th and  $n$ -th unit vectors. Collecting the coefficient vectors  $\mathbf{u}_{\text{loc},h}^\pm(b_{\Gamma_0^\pm, m}, 0)$ ,  $m \in \{1, \dots, N(\Gamma_0^\pm)\}$ , in matrices  $\mathbf{U}_{\text{loc},h,0}^\pm \in \mathbb{C}^{N(C_1^\pm) \times N(\Gamma_0^\pm)}$  satisfying

$$\mathbf{S}_{C_1^\pm}^\varepsilon(\omega, k) \mathbf{U}_{\text{loc},h,0}^\pm = -\mathbf{M}_{C_1^\pm}^{\Gamma_0^\pm}(C_1^\pm, \Gamma_0^\pm),$$

and the coefficient vectors  $\mathbf{u}_{\text{loc},h}^\pm(0, b_{\Gamma_0^\pm, n})$ ,  $n \in \{1, \dots, N(\Gamma_0^\pm)\}$ , in matrices  $\mathbf{U}_{\text{loc},h,1}^\pm \in \mathbb{C}^{N(C_1^\pm) \times N(\Gamma_0^\pm)}$  satisfying

$$\mathbf{S}_{C_1^\pm}^\varepsilon(\omega, k) \mathbf{U}_{\text{loc},h,1}^\pm = -\mathbf{M}_{C_1^\pm}^{\Gamma_1^\pm}(C_1^\pm, \Gamma_1^\pm),$$

we can — using Eq. (3.16) and Eq. (3.17) — deduce

$$\begin{aligned} \mathbf{T}_{\text{fb}}^\pm &= 2i\alpha \mathbf{U}_{\text{loc},h,0}^\pm(\Gamma_0^\pm) - \mathbf{I}, \\ \mathbf{T}_{\text{ff}}^\pm &= 2i\alpha \mathbf{U}_{\text{loc},h,0}^\pm(\Gamma_1^\pm), \\ \mathbf{T}_{\text{bb}}^\pm &= 2i\alpha \mathbf{U}_{\text{loc},h,1}^\pm(\Gamma_0^\pm), \\ \mathbf{T}_{\text{bf}}^\pm &= 2i\alpha \mathbf{U}_{\text{loc},h,1}^\pm(\Gamma_1^\pm) - \mathbf{I}, \end{aligned}$$

where  $\mathbf{U}_{\text{loc},h,i}^\pm(\Gamma_j^\pm)$ ,  $i, j \in \{0, 1\}$ , denotes the block matrix of  $\mathbf{U}_{\text{loc},h,i}^\pm$  with row indices  $\mathcal{J}(C_1^\pm, \Gamma_j^\pm)$ .

The matrices  $\mathbf{T}_{ij}^\pm$ ,  $i, j \in \{\text{f}, \text{b}\}$ , map coefficient vectors of finite element functions in  $S_{\text{per}}^{p,1}(\Gamma_0^\pm)$  onto coefficient vectors of other finite element functions in  $S_{\text{per}}^{p,1}(\Gamma_0^\pm)$ , *i.e.* they map in strong sense. Hence, products of local RtR operators, as they appear



in the Riccati equation (3.9) and the formula (3.11) for the computation of the RtR operator, can be realized by simply multiplying the matrices  $\mathbf{T}_{ij}^\pm$ ,  $i, j \in \{\mathbf{f}, \mathbf{b}\}$ . This is in contrast to the matrices of the local DtN operators in [13], which are computed in weak sense and hence, cannot be multiplied directly.

It remains to show that matrix representation of the inverse  $(\mathcal{J}_{\mathbf{bf},h}^\pm)^{-1}$  of  $\mathcal{J}_{\mathbf{bf},h}^\pm$  is equivalent to the inverse  $(\mathbf{T}_{\mathbf{bf}}^\pm)^{-1}$  of the matrix  $\mathbf{T}_{\mathbf{bf}}^\pm$ . To see this, let us first introduce the matrix  $\tilde{\mathbf{T}}^\pm$  with coefficients  $\tilde{T}_{mn}^\pm$ ,  $m, n \in \{1, \dots, N(\Gamma_0^\pm)\}$ , such that

$$\left(\mathcal{J}_{\mathbf{fb},h}^\pm\right)^{-1} b_{\Gamma_0^\pm,n} = \sum_{m=1}^{N(\Gamma_0^\pm)} \tilde{T}_{mn}^\pm b_{\Gamma_0^\pm,m}. \quad (3.19)$$

Since  $\mathcal{J}_{\mathbf{bf},h}^\pm$  is well-defined and invertible when the finite element space is rich enough, we deduce that

$$\mathcal{J}_{\mathbf{bf},h}^\pm \left(\mathcal{J}_{\mathbf{bf},h}^\pm\right)^{-1} b_{\Gamma_0^\pm,n} = b_{\Gamma_0^\pm,n} \quad \text{and} \quad \left(\mathcal{J}_{\mathbf{bf},h}^\pm\right)^{-1} \mathcal{J}_{\mathbf{bf},h}^\pm b_{\Gamma_0^\pm,n} = b_{\Gamma_0^\pm,n}.$$

Taking Eqs. (3.17) and (3.19) into account, this implies  $\mathbf{T}_{\mathbf{bf}}^\pm \tilde{\mathbf{T}}^\pm = \tilde{\mathbf{T}}^\pm \mathbf{T}_{\mathbf{bf}}^\pm = \mathbf{I}$  and hence,  $\tilde{\mathbf{T}}^\pm = (\mathbf{T}_{\mathbf{bf}}^\pm)^{-1}$ .

To summarize, it is sufficient to solve the block system

$$\begin{pmatrix} \mathbf{S}_{C_1^\pm}^\varepsilon(\omega, k) & \mathbf{0} & \mathbf{0} \\ -2i\alpha\mathbf{I}(\Gamma_0^\pm, C_1^\pm) & \mathbf{I} & \mathbf{0} \\ -2i\alpha\mathbf{I}(\Gamma_1^\pm, C_1^\pm) & \mathbf{0} & \mathbf{I} \end{pmatrix} \begin{pmatrix} \mathbf{U}_{\text{loc},h,0}^\pm & \mathbf{U}_{\text{loc},h,1}^\pm \\ \mathbf{T}_{\mathbf{fb}}^\pm & \mathbf{T}_{\mathbf{bb}}^\pm \\ \mathbf{T}_{\mathbf{ff}}^\pm & \mathbf{T}_{\mathbf{bf}}^\pm \end{pmatrix} = \begin{pmatrix} -\mathbf{M}_{C_1^\pm}^{\Gamma_0^\pm}(C_1^\pm, \Gamma_0^\pm) & -\mathbf{M}_{C_1^\pm}^{\Gamma_1^\pm}(C_1^\pm, \Gamma_1^\pm) \\ -\mathbf{I} & \mathbf{0} \\ \mathbf{0} & -\mathbf{I} \end{pmatrix}$$

for the matrices  $\mathbf{T}_{\mathbf{fb}}^\pm$ ,  $\mathbf{T}_{\mathbf{ff}}^\pm$ ,  $\mathbf{T}_{\mathbf{bb}}^\pm$  and  $\mathbf{T}_{\mathbf{bf}}^\pm$ , where the rectangular matrices  $\mathbf{I}(\Gamma_i^\pm, C_1^\pm) \in \mathbb{R}^{N(\Gamma_0^\pm) \times N(C_1^\pm)}$ ,  $i \in \{0, 1\}$ , are the block matrices of the  $N(C_1^\pm) \times N(C_1^\pm)$  identity matrix with row indices  $\mathcal{J}(C_1^\pm, \Gamma_i^\pm)$ .

### 3.4.3 Solution of the discrete Riccati equation

In this subsection we face the problem of solving the Riccati equation (3.9) in discrete form in order to compute discrete approximations to the forward-forward propagation operators  $\mathcal{P}_{\mathbf{ff}}^\pm(\omega, k)$  and the forward-backward propagation operators  $\mathcal{P}_{\mathbf{fb}}^\pm(\omega, k)$ . In other words, we search for discrete operators  $\mathcal{P}_{\mathbf{ff},h}^\pm(\omega, k) \in \mathcal{L}(S_{\text{per}}^{p,1}(\Gamma_0^\pm))$  with spectral radius strictly smaller than 1 that satisfy the discrete operator equation

$$\begin{aligned} \mathcal{J}_{\mathbf{bb},h}^\pm \left(\mathcal{J}_{\mathbf{bf},h}^\pm\right)^{-1} \left(\mathcal{P}_{\mathbf{ff},h}^\pm\right)^2 + \left(\mathcal{J}_{\mathbf{fb},h}^\pm - \left(\mathcal{J}_{\mathbf{bf},h}^\pm\right)^{-1} - \mathcal{J}_{\mathbf{bb},h}^\pm \left(\mathcal{J}_{\mathbf{bf},h}^\pm\right)^{-1} \mathcal{J}_{\mathbf{ff},h}^\pm\right) \mathcal{P}_{\mathbf{ff},h}^\pm \\ + \left(\mathcal{J}_{\mathbf{bf},h}^\pm\right)^{-1} \mathcal{J}_{\mathbf{ff},h}^\pm = 0, \quad (3.20) \end{aligned}$$

*c.f.* Eq. (3.9). Similarly, we introduce the discrete forward-backward propagation operator  $\mathcal{P}_{\mathbf{fb},h}^\pm(\omega, k) \in \mathcal{L}(S_{\text{per}}^{p,1}(\Gamma_0^\pm))$  by

$$\mathcal{P}_{\mathbf{fb},h}^\pm = \left(\mathcal{J}_{\mathbf{bf},h}^\pm\right)^{-1} \left(\mathcal{P}_{\mathbf{ff},h}^\pm - \mathcal{J}_{\mathbf{ff},h}^\pm\right),$$

*c.f.* Eq. (3.8). Using the basis  $b_{\Gamma_0^\pm, n}$ ,  $n \in \{1, \dots, N(\Gamma_0^\pm)\}$ , of  $S_{\text{per}}^{p,1}(\Gamma_0^\pm)$  we want to express the discrete forward-forward propagation operator  $\mathcal{P}_{\text{ff},h}^\pm$  in matrices  $\mathbf{P}_{\text{ff}}^\pm \in \mathbb{C}^{N(\Gamma_0^\pm) \times N(\Gamma_0^\pm)}$  with coefficients  $P_{\text{ff},mn}^\pm$ ,  $m, n \in \{1, \dots, N(\Gamma_0^\pm)\}$ , that satisfy

$$\mathcal{P}_{\text{ff},h}^\pm \boldsymbol{\varphi}_h^\pm(\mathbf{x}) = \sum_{n=1}^{N(\Gamma_0^\pm)} \boldsymbol{\varphi}_n^\pm \sum_{m=1}^{N(\Gamma_0^\pm)} P_{\text{ff},mn}^\pm b_{\Gamma_0^\pm, m}(\mathbf{x}). \quad (3.21)$$

Using this definition and the definition of the matrices  $\mathbf{T}_{ij}^\pm$ ,  $i, j \in \{\text{f}, \text{b}\}$ , in (3.17) we can write Eq. (3.20) as a quadratic matrix-valued equation

$$\mathbf{T}_{\text{bb}}^\pm (\mathbf{T}_{\text{bf}}^\pm)^{-1} (\mathbf{P}_{\text{ff}}^\pm)^2 + \left( \mathbf{T}_{\text{fb}}^\pm - (\mathbf{T}_{\text{bf}}^\pm)^{-1} - \mathbf{T}_{\text{bb}}^\pm (\mathbf{T}_{\text{bf}}^\pm)^{-1} \mathbf{T}_{\text{ff}}^\pm \right) \mathbf{P}_{\text{ff}}^\pm + (\mathbf{T}_{\text{bf}}^\pm)^{-1} \mathbf{T}_{\text{ff}}^\pm = \mathbf{0}. \quad (3.22)$$

Considering that the discretization preserves the periodicity properties of  $C_1^\pm$  in  $\mathbf{a}_2$ -direction we deduce that the forward-forward propagation matrix  $\mathbf{P}_{\text{ff}}^\pm$  is the unique matrix satisfying Eq. (3.22) with eigenvalues whose magnitudes are strictly less than 1.

Analogously to [13] for the computation of the discrete Dirichlet propagation operator, we propose a spectral decomposition to compute  $\mathbf{P}_{\text{ff}}^\pm$ . Even though we cannot guarantee that  $\mathbf{P}_{\text{ff}}^\pm$  is diagonalizable the spectral decomposition has proven to be an efficient and reliable approach to compute  $\mathbf{P}_{\text{ff}}^\pm$ . If, however, the propagation matrix  $\mathbf{P}_{\text{ff}}^\pm$  is in fact of Jordan type and hence, cannot be diagonalized, we can still use this spectral method in a generalized form by identifying the Jordan blocks and computing the Jordan chains, as shown in [4] for the DtN method.

Thus, we want to find eigenvalues  $\mu^\pm(\boldsymbol{\omega}, k) \in \mathbb{C}$  with magnitude strictly less than 1 and their corresponding eigenvectors  $\boldsymbol{\psi}^\pm(\boldsymbol{\omega}, k) \in \mathbb{C}^{N(\Gamma_0^\pm)}$  of the quadratic eigenvalue problem

$$\left[ \mathbf{T}_{\text{bb}}^\pm (\mathbf{T}_{\text{bf}}^\pm)^{-1} (\mu^\pm)^2 + \left( \mathbf{T}_{\text{fb}}^\pm - (\mathbf{T}_{\text{bf}}^\pm)^{-1} - \mathbf{T}_{\text{bb}}^\pm (\mathbf{T}_{\text{bf}}^\pm)^{-1} \mathbf{T}_{\text{ff}}^\pm \right) \mu^\pm + (\mathbf{T}_{\text{bf}}^\pm)^{-1} \mathbf{T}_{\text{ff}}^\pm \right] \boldsymbol{\psi}^\pm = \mathbf{0}, \quad (3.23)$$

which can be transformed into the generalized linear eigenvalue problem

$$\begin{pmatrix} - \left( \mathbf{T}_{\text{fb}}^\pm - (\mathbf{T}_{\text{bf}}^\pm)^{-1} - \mathbf{T}_{\text{bb}}^\pm (\mathbf{T}_{\text{bf}}^\pm)^{-1} \mathbf{T}_{\text{ff}}^\pm \right) & - (\mathbf{T}_{\text{bf}}^\pm)^{-1} \mathbf{T}_{\text{ff}}^\pm \\ \mathbf{I} & \mathbf{0} \end{pmatrix} \boldsymbol{\Psi}^\pm = \mu^\pm \begin{pmatrix} \mathbf{T}_{\text{bb}}^\pm (\mathbf{T}_{\text{bf}}^\pm)^{-1} \mathbf{0} \\ \mathbf{0} & \mathbf{I} \end{pmatrix} \boldsymbol{\Psi}^\pm, \quad (3.24)$$

*c.f.* [19], with  $\boldsymbol{\Psi}^\pm = \begin{pmatrix} \mu^\pm \boldsymbol{\psi}^\pm \\ \boldsymbol{\psi}^\pm \end{pmatrix}$ .

Now let us present an important result of the spectral decomposition. If  $\boldsymbol{\omega}^2 \in \mathbb{R}^+ \setminus \sigma_{\text{ess}}(k)$  is not a global or local Dirichlet eigenvalue, *i.e.* an eigenvalue of the infinite half-strip problem (3.1a) or the local cell problem (3.3a) with homogeneous Dirichlet boundary conditions, the following result is a direct consequence of Proposition 3.2 and Proposition 5.2 in [13]. If, however,  $\boldsymbol{\omega}^2$  is such a global or local Dirichlet eigenvalue we conjecture that the result still holds true.

1  
2 *Conjecture 3.1* If  $\mu^\pm(\omega, k) \in \mathbb{C} \setminus \{0\}$  is an eigenvalue of (3.23), then  $(\overline{\mu^\pm(\omega, k)})^{-1}$   
3 is also an eigenvalue.  
4

5 As a by-product and analogously to the case with DtN operators [13], the spectral  
6 decomposition of the propagation matrix  $\mathbf{P}_{\text{ff}}^\pm(\omega, k)$  yields the information whether  
7  $\omega^2$  is inside the discrete approximation of the essential spectrum  $\sigma_{\text{ess}}(k)$ .  
8

9 **Definition 3.1** We call the approximative essential spectrum  $\sigma_{\text{ess},h}^\pm(k)$  the set of num-  
10 bers  $\omega^2$  for which the quadratic eigenvalue problem (3.23) has eigenvalues with mag-  
11 nitude 1. Furthermore, we define  $\sigma_{\text{ess},h}(k) := \sigma_{\text{ess},h}^+(k) \cup \sigma_{\text{ess},h}^-(k)$ .  
12  
13

14 With the help of Conjecture 3.1 and Definition 3.1 it is now clear how to compute  
15 the spectral decomposition of the propagation matrix  $\mathbf{P}_{\text{ff}}^\pm(\omega, k)$ . We solve the gen-  
16 eral eigenvalue problem (3.24) for its  $2N(\Gamma_0^\pm)$  eigenvalues  $\mu^\pm(\omega, k)$ . If there exist  
17 eigenvalues with magnitude equal to 1 we stop our computation as we know from  
18 Definition 3.1 that this means that  $\omega^2$  is in the approximative essential spectrum  
19  $\sigma_{\text{ess},h}(k)$ . Otherwise, and in accordance to Conjecture 3.1, the  $2N(\Gamma_0^\pm)$  eigenvalues  
20  $\mu^\pm(\omega, k)$  split into  $N(\Gamma_0^\pm)$  eigenvalues with magnitude strictly less than 1 and  $N(\Gamma_0^\pm)$   
21 eigenvalues with magnitude strictly larger than 1. While discarding the  $N(\Gamma_0^\pm)$  eigen-  
22 values with magnitude strictly larger than 1, the  $N(\Gamma_0^\pm)$  eigenvalues  $\mu^\pm(\omega, k)$  with  
23 magnitude strictly less than 1 and their corresponding eigenvectors  $\psi^\pm(\omega, k)$  form  
24 the spectral decomposition of the propagation matrix  $\mathbf{P}_{\text{ff}}^\pm(\omega, k)$ .  
25  
26

#### 27 3.4.4 Definition of the discrete Robin-to-Robin operators

28 Considering the definition (3.2) of the RtR operators  $\mathcal{R}^\pm(\omega, k)$  applied to some for-  
29 ward Robin trace  $\varphi \in H_{\text{per}}^{-1/2}(\Gamma_0^\pm)$ , we define the discrete RtR operators  $\mathcal{R}_h^\pm(\omega, k) \in$   
30  $\mathcal{L}(S_{\text{per}}^{p,1}(\Gamma_0^\pm))$  by  
31  
32

$$33 \mathcal{R}_h^\pm(\omega, k) \varphi_h = (\mp \partial_2 + i\alpha) u_{\text{loc},h}(\cdot; \omega, k, \varphi_h, \mathcal{P}_{\text{fb},h}(\omega, k) \varphi_h) |_{\Gamma_0^\pm}$$

34 for any  $\varphi_h \in S_{\text{per}}^{p,1}(\Gamma_0^\pm)$ , and hence — using the matrix representations of the discrete  
35 local RtR operators and the discrete propagation operators — we can compute RtR  
36 matrices  $\mathbf{R}^\pm(\omega, k) \in \mathbb{C}^{N(\Gamma_0^\pm) \times N(\Gamma_0^\pm)}$  with entries  $R_{mn}^\pm$ ,  $m, n \in \{1, \dots, N(\Gamma_0^\pm)\}$ , that sat-  
37 isfy  
38  
39  
40  
41

$$42 \mathcal{R}_h^\pm(\omega, k) b_{\Gamma_0^\pm, n} = \sum_{m=1}^{N(\Gamma_0^\pm)} R_{mn}^\pm b_{\Gamma_0^\pm, m},$$

43 such that  
44  
45

$$46 \mathbf{R}^\pm = \mathbf{T}_{\text{fb}}^\pm + \mathbf{T}_{\text{bb}}^\pm (\mathbf{T}_{\text{bf}}^\pm)^{-1} \mathbf{P}_{\text{ff}} - \mathbf{T}_{\text{bb}}^\pm (\mathbf{T}_{\text{bf}}^\pm)^{-1} \mathbf{T}_{\text{ff}}^\pm,$$

47 c. f. Eq. (3.11).  
48  
49  
50  
51  
52  
53  
54  
55  
56  
57  
58  
59  
60  
61  
62  
63  
64  
65

## 4 Non-linear eigenvalue problem on a bounded domain

In the previous section we introduced RtR operators for periodic media, explained their computation and discretization. In this section we now want to show how to employ these operators in order to transform the linear (or quadratic) eigenvalue problem (2.3) on the unbounded domain  $S$  to a non-linear eigenvalue problem posed on the defect cell  $C_0$ . We will start with the problem in strong formulation. After introducing a variational formulation, we will elaborate on the discretization of this non-linear eigenvalue problem and finally, we present numerical solution techniques to solve the non-linear eigenvalue problem in discretized form.

### 4.1 Main theorem

We start with the main result of the RtR method [4].

**Theorem 4.1** *The eigenvalue problem (2.3) posed on the unbounded domain  $S$  is equivalent to: find eigenvalue couples  $(\omega^2, k) \in \mathbb{R}^+ \times B$ , with  $\omega^2 \notin \sigma_{\text{ess}}(k)$ , such that there exists a non-trivial  $u \in H_{\text{per}}^1(\Delta, C_0)$  that satisfies*

$$-(\nabla + ika_1) \cdot (\nabla + ika_1)u - \omega^2 \varepsilon u = 0 \quad \text{in } C_0, \quad (4.1a)$$

$$(\mp \partial_2 + i\alpha)u = \mathcal{R}^\pm(\omega, k)(\pm \partial_2 + i\alpha)u \quad \text{on } \Gamma_0^\pm. \quad (4.1b)$$

Note that the problem (4.1) — in comparison to problem (2.3) — is posed on the bounded domain  $C_0$  but it is non-linear with respect to  $\omega$  and  $k$  due to the dependence of the RtR operators on  $\omega$  and  $k$ .

### 4.2 Variational formulation of the non-linear eigenvalue problem

#### 4.2.1 Mixed variational formulation

In order to derive a variational formulation of the non-linear eigenvalue problem (4.1) with RtR operators, we introduce Lagrangian multipliers  $\lambda^\pm \in H_{\text{per}}^{-1/2}(\Gamma_0^\pm)$  defined by

$$\lambda^\pm = \pm \partial_2 u|_{\Gamma_0^\pm}$$

for the Neumann trace on  $\Gamma_0^\pm$ . Using the linearity of the RtR operators, we deduce that a mixed variational formulation of the non-linear eigenvalue problem (4.1) is to find eigenvalue couples  $(\omega^2, k) \in \mathbb{R}^+ \times B$  with  $\omega^2 \notin \sigma_{\text{ess}}(k)$ , and associated eigenmodes

$(u, \lambda^+, \lambda^-) \in H_{\text{per}}^1(C_0) \times H_{\text{per}}^{-1/2}(\Gamma_0^+) \times H_{\text{per}}^{-1/2}(\Gamma_0^-)$  such that

$$\int_{C_0} (\nabla + i\mathbf{k}\mathbf{a}_1)u \cdot (\nabla - i\mathbf{k}\mathbf{a}_1)\bar{v} - \omega^2 \varepsilon u \bar{v} \, d\mathbf{x} - \int_{\Gamma_0^+} \lambda^+ \bar{v} \, ds(\mathbf{x}) - \int_{\Gamma_0^-} \lambda^- \bar{v} \, ds(\mathbf{x}) = 0, \quad (4.2a)$$

$$i\alpha \int_{\Gamma_0^+} (\mathcal{J} - \mathcal{R}^+(\omega, k))u \overline{\psi^+} \, ds(\mathbf{x}) - \int_{\Gamma_0^+} (\mathcal{J} + \mathcal{R}^+(\omega, k))\lambda^+ \overline{\psi^+} \, ds(\mathbf{x}) = 0, \quad (4.2b)$$

$$i\alpha \int_{\Gamma_0^-} (\mathcal{J} - \mathcal{R}^-(\omega, k))u \overline{\psi^-} \, ds(\mathbf{x}) - \int_{\Gamma_0^-} (\mathcal{J} + \mathcal{R}^-(\omega, k))\lambda^- \overline{\psi^-} \, ds(\mathbf{x}) = 0, \quad (4.2c)$$

for all  $(v, \psi^+, \psi^-) \in H_{\text{per}}^1(C_0) \times H_{\text{per}}^{-1/2}(\Gamma_0^+) \times H_{\text{per}}^{-1/2}(\Gamma_0^-)$ , where  $\mathcal{J}$  denotes the identity operator.

#### 4.2.2 Variational formulation with Dirichlet-to-Neumann operators

Now we aim to derive an alternative variational formulation which employs DtN operators and which is — in contrast to the mixed variational formulation (4.2) — symmetric with respect to the trial and test spaces. However, this formulation is not well-posed at all frequencies in the band gap as one has to exclude the global Dirichlet eigenvalues.

First, we recall that the RtR operators  $\mathcal{R}^\pm(\omega, k)$  are linear, and hence, we can rewrite the Robin boundary condition (4.1b) in the form

$$(\mathcal{J} + \mathcal{R}^\pm(\omega, k)) \left( \pm \partial_2 u|_{\Gamma_0^\pm} \right) = i\alpha (\mathcal{J} - \mathcal{R}^\pm(\omega, k))u|_{\Gamma_0^\pm}. \quad (4.3)$$

Then we present an important result [4] on the operator  $(\mathcal{J} + \mathcal{R}^\pm(\omega, k))$ , which also appears in Eqs. (4.2b)–(4.2c), where it is applied to the Lagrangian multipliers  $\lambda^\pm$ .

**Proposition 4.1** *Let  $k \in B$  and  $\omega^2 \in \mathbb{R}^+ \setminus \sigma_{\text{ess}}(k)$ . Furthermore, we assume that  $\omega^2$  is not a global Dirichlet eigenvalue, i. e. an eigenvalue of the infinite half-strip problem (3.1a) with homogeneous Dirichlet boundary condition (3.10). Then the operator  $(\mathcal{J} + \mathcal{R}^\pm(\omega, k))$  is invertible.*

*Proof* By definition of the RtR operator and the Robin problems in the infinite half-strips, the operator  $(\mathcal{J} + \mathcal{R}^\pm(\omega, k)) \in \mathcal{L}(H_{\text{per}}^{-1/2}(\Gamma_0^\pm))$  is given by

$$(\mathcal{J} + \mathcal{R}^\pm(\omega, k)) \varphi = 2i\alpha u^\pm(\cdot; \omega, k, \varphi)|_{\Gamma_0^\pm},$$

where  $u^\pm(\cdot; \omega, k, \varphi)$  is the unique solution of (3.1). Using the same ideas as in Lemma 3.1, we can show that for any  $\varphi_{\text{DtN}} \in H_{\text{per}}^{-1/2}(\Gamma_0^\pm)$  the inverse of  $(\mathcal{J} + \mathcal{R}^\pm(\omega, k))$  is defined by

$$\varphi_{\text{DtN}} \in H_{\text{per}}^{-1/2}(\Gamma_0^\pm) \mapsto \frac{(\pm \partial_2 + i\alpha)}{2i\alpha} u_{\text{DtN}}^\pm(\varphi_{\text{DtN}})|_{\Gamma_0^\pm},$$

where  $u_{\text{DtN}}^\pm(\varphi_{\text{DtN}})$  is the unique solution (because  $\omega^2$  is assumed to be not in the set of global Dirichlet eigenvalues) of (3.1a) with boundary condition (3.10).  $\square$

Using Proposition 4.1 and Eq. (4.3), we can deduce that the Robin boundary condition (4.1b) is equivalent to the Neumann boundary condition

$$\pm \partial_2 u|_{\Gamma_0^\pm} = \mathcal{D}^\pm(\omega, k)u|_{\Gamma_0^\pm}$$

with the DtN operator

$$\mathcal{D}^\pm(\omega, k) = i\alpha(\mathcal{J} + \mathcal{R}^\pm(\omega, k))^{-1}(\mathcal{J} - \mathcal{R}^\pm(\omega, k)), \quad (4.4)$$

if  $\omega^2$  is not a global Dirichlet eigenvalue.

Then the derivation of the corresponding weak formulation of the problem with DtN operators is straightforward: find eigenvalue couples  $(\omega^2, k) \in \mathbb{R}^+ \times B$ , with  $\omega^2 \notin \sigma_{\text{ess}}(k)$ , and associated eigenmodes  $u \in H_{\text{per}}^1(C_0)$  such that

$$\begin{aligned} \int_{C_0} (\nabla + i k \mathbf{a}_1)u \cdot (\nabla - i k \mathbf{a}_1)\bar{v} - \omega^2 \varepsilon u \bar{v} \, d\mathbf{x} \\ - \int_{\Gamma_0^+} \mathcal{D}^+(\omega, k)u|_{\Gamma_0^+} \bar{v} \, ds(\mathbf{x}) - \int_{\Gamma_0^-} \mathcal{D}^-(\omega, k)u|_{\Gamma_0^-} \bar{v} \, ds(\mathbf{x}) = 0 \end{aligned} \quad (4.5)$$

for all  $v \in H_{\text{per}}^1(C_0)$ .

*Remark 4.1* Let  $k \in B$  and  $\omega^2 \in \mathbb{R}^+ \setminus \sigma_{\text{ess}}(k)$ . Furthermore, let us assume that  $\omega^2$  is not a global Dirichlet eigenvalue, *i. e.* an eigenvalue of the infinite half-strip problem (3.1a) with homogeneous Dirichlet boundary condition (3.10). Then the DtN operator  $\mathcal{D}^\pm(\omega, k)$  is well-defined and can be computed according to Eq. (4.4). If, additionally,  $\omega^2$  is not equal to a local Dirichlet eigenvalue, *i. e.* an eigenvalue of the local cell problem (3.3a), then the DtN operator based on the DtN approach as described in [5, 13], that we will denote here by  $\mathcal{D}_{\text{DtN}}^\pm(\omega, k)$ , exists and is well-defined. This implies — according to Theorem 4.1 and its analogon for the DtN approach [5] — that  $\mathcal{D}^\pm(\omega, k) = \mathcal{D}_{\text{DtN}}^\pm(\omega, k)$  for all  $(\omega^2, k) \in \mathbb{R}^+ \times B$  with  $\omega^2 \notin \sigma_{\text{ess}}(k)$  except for a countable set of frequencies — the global and local Dirichlet eigenvalues.

#### 4.3 Discretization of the non-linear eigenvalue problem

Now let us elaborate on the discretization of the variational formulations introduced above. We recall the finite element space  $S_{\text{per}}^{p,1}(\Gamma_0^\pm)$  introduced as discrete subspace of  $H_{\text{per}}^{1/2}(\Gamma_0^\pm)$  in Section 3.4. Furthermore, recall that we assumed in Section 3.4 that there is no jump of the material coefficient on the boundaries  $\Gamma_0^\pm$  which implies that the Neumann and Robin traces on  $\Gamma_0^\pm$  are in  $H_{\text{per}}^{1/2}(\Gamma_0^\pm)$  and hence, we shall take  $S_{\text{per}}^{p,1}(\Gamma_0^\pm)$  as discrete subspace of  $H_{\text{per}}^{-1/2}(\Gamma_0^\pm)$ . Then, we additionally introduce  $S_{\text{per}}^{p,1}(C_0)$  as the finite element subspaces of  $H_{\text{per}}^1(C_0)$  with  $N(C_0) = \dim S_{\text{per}}^{p,1}(C_0)$ .

Similarly to the choice of the basis functions of  $S_{\text{per}}^{p,1}(C_1^\pm)$ , we order the basis functions  $b_{C_0,n}$ ,  $n \in \mathcal{J}(C_0) = \{1, \dots, N(C_0)\}$  of the finite element space  $S_{\text{per}}^{p,1}(C_0)$  such that

- the basis functions of  $S_{\text{per}}^{p,1}(C_0)$  with index  $n \in \mathcal{J}(C_0, \Gamma_0^+) = \{1, \dots, N(\Gamma_0^+)\}$  vanish on  $\Gamma_0^-$  and build a basis of  $S_{\text{per}}^{p,1}(\Gamma_0^+)$ ,
- the basis functions of  $S_{\text{per}}^{p,1}(C_0)$  with index  $n \in \mathcal{J}(C_0, \Gamma_0^-) = \{N(\Gamma_0^+) + 1, \dots, N(\Gamma_0^+) + N(\Gamma_0^-)\}$  vanish on  $\Gamma_0^+$  and build a basis of  $S_{\text{per}}^{p,1}(\Gamma_0^-)$ , and
- the basis functions of  $S_{\text{per}}^{p,1}(C_0)$  with index  $n \in \mathcal{J}(C_0) \setminus (\mathcal{J}(C_0, \Gamma_0^+) \cup \mathcal{J}(C_0, \Gamma_0^-)) = \{N(\Gamma_0^+) + N(\Gamma_0^-) + 1, \dots, N(C_0)\}$  vanish on  $\Gamma_0^+$  and  $\Gamma_0^-$ .

With this special ordering of the basis functions we introduce permutation matrices  $\mathbf{Q}_{C_0}^- \in \mathbb{R}^{N(\Gamma_0^-) \times N(\Gamma_0^-)}$  and  $\mathbf{Q}_{C_0}^+ \in \mathbb{R}^{N(\Gamma_0^+) \times N(\Gamma_0^+)}$  such that

$$b_{\Gamma_0^-, n} = \sum_{m=1}^{N(\Gamma_0^-)} \mathcal{Q}_{C_0, mn}^- b_{C_0, m}|_{\Gamma_0^-}, \quad (4.6a)$$

$$b_{\Gamma_0^+, n} = \sum_{m=1}^{N(\Gamma_0^+)} \mathcal{Q}_{C_0, mn}^+ b_{C_0, N(\Gamma_0^-) + m}|_{\Gamma_0^+}. \quad (4.6b)$$

For simplicity of notation we shall again assume that the basis functions of  $S_{\text{per}}^{p,1}(C_0)$  and  $S_{\text{per}}^{p,1}(\Gamma_0^\pm)$  are ordered such that the permutation matrices are identity matrices of size  $N(\Gamma_0^\pm) \times N(\Gamma_0^\pm)$ .

Analogously to the discretization of the local cell problems, let  $\mathbf{A}_{C_0}(k) \in \mathbb{C}^{N(C_0) \times N(C_0)}$  denote the matrix with coefficients

$$A_{C_0, mn}(k) = \int_{C_0} (\nabla + i k \mathbf{a}_1) b_{C_0, n} \cdot (\nabla - i k \mathbf{a}_1) \bar{b}_{C_0, m} \, d\mathbf{x},$$

$m, n \in \{1, \dots, N(C_0)\}$ , *c.f.* Eq. (4.2a). Similarly, let  $\mathbf{M}_{C_0}^\varepsilon \in \mathbb{R}^{N(C_0) \times N(C_0)}$  denote the matrix with coefficients

$$M_{C_0, mn}^\varepsilon = \int_{C_0} \varepsilon b_{C_0, n} \bar{b}_{C_0, m} \, d\mathbf{x},$$

$m, n \in \{1, \dots, N(C_0)\}$ , *c.f.* Eq. (4.2a). Moreover, we introduce the matrices  $\mathbf{M}_{C_0}^{\Gamma_0^\pm} \in \mathbb{R}^{N(C_0) \times N(C_0)}$  with coefficients

$$M_{C_0, mn}^{\Gamma_0^\pm}(k) = \int_{\Gamma_0^\pm} b_{C_0, n} \bar{b}_{C_0, m} \, ds(\mathbf{x}),$$

$m, n \in \{1, \dots, N(C_0)\}$ , related to the boundary integrals in Eq. (4.2). Then we define  $\mathbf{M}_{C_0}^{\Gamma_0^\pm}(O_1, O_2)$  as the block matrix of  $\mathbf{M}_{C_0}^{\Gamma_0^\pm}$  with row indices  $\mathcal{J}(C_0, O_1)$  and column indices  $\mathcal{J}(C_0, O_2)$ .

With these definitions and the special ordering of the basis functions  $b_{C_0, n}$  of the space  $S_{\text{per}}^{p,1}(C_0)$  described above, the discretization of the mixed variational formula-

tion (4.2) reads

$$\begin{pmatrix} \mathbf{A}_{C_0}(k) - \omega^2 \mathbf{M}_{C_0}^\varepsilon & \mathbf{M}_{C_0}^{\Gamma_0^+}(C_0, \Gamma_0^+) & \mathbf{M}_{C_0}^{\Gamma_0^-}(C_0, \Gamma_0^-) \\ i\alpha \mathbf{M}_{C_0}^{\Gamma_0^+}(\Gamma_0^+, C_0)(\mathbf{I} - \mathbf{R}^+) & -\mathbf{M}_{C_0}^{\Gamma_0^+}(\Gamma_0^+, \Gamma_0^+)(\mathbf{I} + \mathbf{R}^+) & \mathbf{0} \\ i\alpha \mathbf{M}_{C_0}^{\Gamma_0^-}(\Gamma_0^-, C_0)(\mathbf{I} - \mathbf{R}^-) & \mathbf{0} & -\mathbf{M}_{C_0}^{\Gamma_0^-}(\Gamma_0^-, \Gamma_0^-)(\mathbf{I} + \mathbf{R}^-) \end{pmatrix} \begin{pmatrix} \mathbf{u}_h \\ \lambda_h^+ \\ \lambda_h^- \end{pmatrix} = \mathbf{0}, \quad (4.7)$$

where  $\mathbf{u}_h \in \mathbb{C}^{N(C_0)}$  is the coefficient vector of the discrete eigenmode  $u_h(\cdot; \omega, k) \in S_{\text{per}}^{p,1}(C_0)$  with respect to the basis functions  $b_{C_0, n}$  of  $S_{\text{per}}^{p,1}(C_0)$ , and  $\lambda_h^\pm \in \mathbb{C}^{N(\Gamma_0^\pm)}$  are the coefficient vectors of the discrete Lagrangian multipliers  $\lambda_h^\pm = \pm \partial_2 u_h|_{\Gamma_0^\pm} \in S_{\text{per}}^{p,1}(\Gamma_0^\pm)$  with respect to the basis functions  $b_{\Gamma_0^\pm, n}$  of  $S_{\text{per}}^{p,1}(\Gamma_0^\pm)$ .

If we choose the variational formulation (4.5) with DtN operators instead of the mixed variational formulation (4.2) we obtain the discrete equation

$$\left( \mathbf{A}_{C_0}(k) - \omega^2 \mathbf{M}_{C_0}^\varepsilon - \mathbf{D}_{C_0}(\omega, k) \right) \mathbf{u}_h = \mathbf{0}, \quad (4.8)$$

where the matrix  $\mathbf{D}_{C_0}(\omega, k) \in \mathbb{C}^{N(C_0) \times N(C_0)}$  is given by

$$\mathbf{D}_{C_0} = \begin{pmatrix} \mathbf{D}_{C_0}^+ & \mathbf{0} & \mathbf{0} \\ \mathbf{0} & \mathbf{D}_{C_0}^- & \mathbf{0} \\ \mathbf{0} & \mathbf{0} & \mathbf{0} \end{pmatrix}$$

with

$$\mathbf{D}_{C_0}^\pm = i\alpha \mathbf{M}_{C_0}^{\Gamma_0^\pm}(\Gamma_0^\pm, \Gamma_0^\pm)(\mathbf{I} + \mathbf{R}^\pm)^{-1}(\mathbf{I} - \mathbf{R}^\pm). \quad (4.9)$$

#### 4.4 Numerical solution of the non-linear eigenvalue problem

The numerical techniques to solve the discretized non-linear eigenvalue problem (4.7) or (4.8) can be split into direct methods and iterative methods. A direct method that is based on a Chebyshev interpolation of the non-linear operator was introduced in [13] for the non-linear eigenvalue problem with DtN operators. Applying this approach to the discretized forms (4.7) and (4.8) of the non-linear eigenvalue problem (4.1) with RtR operators is straightforward.

Also in [13] a Newton's method was introduced as representative of the class of iterative methods. Now we will apply this method to the solution of the non-linear eigenvalue problem (4.1). For simplicity, let us only consider the  $\omega$ -formulation, where we fix the quasi-momentum  $k$  and search for eigenvalues  $\omega$  of the non-linear eigenvalue problem (4.1). The iterative method for the  $k$ -formulation can be deduced analogously.

First, we introduce a "simplified" eigenvalue problem, which can be obtained from the non-linear eigenvalue problem (4.1) by fixing the  $(\omega, k)$ -dependent RtR



operators. To this end, let  $\omega_{\mathcal{R}}^2 \in \mathbb{R}^+ \setminus \sigma_{\text{ess}}(k)$  be arbitrary but fixed. Then the problem

$$-(\nabla + ika_1) \cdot (\nabla + ika_1)u - \omega^2 \varepsilon u = 0 \quad \text{in } C_0, \quad (4.10a)$$

$$(\mp \partial_2 + i\alpha)u = \mathcal{R}^\pm(\omega_{\mathcal{R}}, k)(\pm \partial_2 + i\alpha)u \quad \text{on } \Gamma_0^\pm. \quad (4.10b)$$

is a linear eigenvalue problem in  $\omega^2$ . If  $\omega^2$  is an eigenvalue of (4.10) with  $\omega = \omega_{\mathcal{R}}$ , then  $(\omega^2, k)$  is an eigenvalue couple of the non-linear eigenvalue problem (4.1).

Now let us repeat some properties of this simplified eigenvalue problem. These results were shown in [5] for the case with DtN operators, but their analogon for the case with RtR operators can be deduced directly, due to the equivalence of the DtN and RtR approach in the sense of Eq. (4.4) and Remark 4.1. However, note that this equivalence holds true at all frequencies inside the band gaps except for a countable set of frequencies — the global and local Dirichlet eigenvalues, *i. e.* the eigenvalues of the infinite half-strip problem (3.1a) with homogeneous Dirichlet boundary conditions, and the eigenvalues of the local cell problem (3.3a) with homogeneous Dirichlet boundary conditions, respectively. Our conjecture is that the following statements also hold true at these global and local Dirichlet eigenvalues.

*Conjecture 4.1* Let  $(\omega_{\mathcal{R}}^2, k) \in \mathbb{R}^+ \times B$  and  $\omega_{\mathcal{R}}^2 \notin \sigma_{\text{ess}}(k)$ . Then the linear eigenvalue problem (4.10) in  $\omega$ -formulation only has a countable set of eigenvalues  $\omega_m^2(\omega_{\mathcal{R}}, k)$ ,  $m \in \mathbb{N}$ . Moreover, these eigenvalues are real.

*Conjecture 4.2* Let  $\omega_m^2(\omega_{\mathcal{R}}, k) \in \mathbb{R}$ ,  $m \in \mathbb{N}$ , denote the eigenvalues of the linear eigenvalue problem (4.10) in  $\omega$ -formulation with  $\omega_m^2 \leq \omega_{m+1}^2$  for all  $m \in \mathbb{N}$ . Then the functions  $g_m^{(1)}(\omega_{\mathcal{R}}, k) = \omega_m^2(\omega_{\mathcal{R}}, k)$  are continuous.

*Conjecture 4.3* There exists an alternative ordering  $m \mapsto \tilde{m}(m)$  of the eigenvalues  $\omega_m^2(\omega_{\mathcal{R}}, k) \in \mathbb{R}$ ,  $m \in \mathbb{N}$ , of the linear eigenvalue problem (4.10) in  $\omega$ -formulation such that the functions  $g_m^{(2)}(\omega_{\mathcal{R}}, k) = \omega_{\tilde{m}(m)}^2(\omega_{\mathcal{R}}, k)$  are continuously differentiable.

With these results we define the distance function of the first kind

$$d_{\omega, m}^{(1)}(\omega_{\mathcal{R}}, k) = \omega_{\mathcal{R}}^2 - g_m^{(1)}(\omega_{\mathcal{R}}, k) = \omega_{\mathcal{R}}^2 - \omega_m^2(\omega_{\mathcal{R}}, k),$$

which is continuous for all  $m \in \mathbb{N}$ . Furthermore, we introduce the distance function of the second kind

$$d_{\omega, m}^{(2)}(\omega_{\mathcal{R}}, k) = \omega_{\mathcal{R}}^2 - g_m^{(2)}(\omega_{\mathcal{R}}, k) = \omega_{\mathcal{R}}^2 - \omega_{\tilde{m}(m)}^2(\omega_{\mathcal{R}}, k),$$

which is continuously differentiable for all  $m \in \mathbb{N}$ . Roots of these functions are eigenvalues of the non-linear eigenvalue problem (4.2).

Analogously to [13] we apply the Newton's method to the global distance function

$$d_{\omega}(\omega_{\mathcal{R}}, k) = d_{\omega, m^*}^{(2)}(\omega_{\mathcal{R}}, k) \quad (4.11)$$

where

$$m^* = \arg \min_{m \in \mathbb{N}} |d_{\omega, m}^{(2)}(\omega_{\mathcal{R}}, k)|,$$

for which differentiability cannot be guaranteed but which delivers reasonable numerical results and saves computational effort since we only have to apply the Newton's method to  $d_\omega(\cdot, k)$  instead of to the first  $M \in \mathbb{N}$  distance functions  $d_{\omega, m}^{(2)}(\cdot, k)$ ,  $m = 1, \dots, M$ .

In [13] we showed the differentiability of the DtN operators and the computation of the derivatives of the DtN operators. We employed these derivatives to compute the derivative of  $d_{\omega, m^*}^{(2)}(\cdot, k)$  that we need in order to apply the Newton's method to the global distance function  $d_\omega(\cdot, k)$ . In this work, we shall for simplicity use a quasi Newton method and approximate the derivative of the global distance function  $d_\omega(\cdot, k)$  by a first order difference quotient.

## 5 Numerical examples

In the numerical examples we want to study the performance of the RtR method in comparison to the DtN method [13] when applied to the computation of eigenvalues that are close to local or global Dirichlet eigenvalues. The DtN operators are not well-defined at global Dirichlet eigenvalues and their computation using Dirichlet cell problems is not stable at local Dirichlet eigenvalues. Therefore, we expect that the DtN method will produce numerical errors when computing eigenvalues close to Dirichlet eigenvalues.

### 5.1 Computation of eigenvalues close to local Dirichlet eigenvalues

In our first numerical example we analyse the behaviour of the quasi Newton method close to a local Dirichlet eigenvalue, *i. e.* an eigenvalue of the local cell problem (3.3a) with homogeneous Dirichlet boundary conditions. We want to study the convergence of the quasi Newton method applied to the proposed non-linear eigenvalue problem with RtR maps and applied to the non-linear eigenvalue problem with DtN transparent boundary conditions as introduced in [13]. For the reasons explained above, we expect a poor convergence of the DtN method and a good convergence of the RtR method.

We shall consider the TE mode in a PhC wave-guide with hexagonal lattice, *i. e.*  $\mathbf{a}_1^0 = \mathbf{a}_1^+ = \mathbf{a}_1^- = (1, 0)^T$  and  $\mathbf{a}_2^0 = \mathbf{a}_2^+ = \mathbf{a}_2^- = (0.5, \sqrt{0.75})^T$ , and with air holes ( $\varepsilon = 1$ ) of radius 0.31 in a homogeneous and isotropic dielectric material of relative permittivity  $\varepsilon = 11.4$ .

For the computation we choose finite elements on curved cells with polynomial degree  $p = 5$  using the C++ library *Concepts* [9, 17, 3].

For orientation we show in Figure 5.1 the magnitude of the global distance function  $d_\omega$  for the chosen configuration. The dark lines indicate small values of  $|d_\omega|$  and therefore represent the eigenvalues of the non-linear eigenvalue problem (4.1). The green lines, on the other hand, show the local Dirichlet eigenvalues, *i. e.* the eigenvalues of the local cell problem (3.3a) with homogeneous Dirichlet boundary conditions. In Figure 5.2 we present the convergence of the quasi Newton method to the common eigenvalue  $\omega \approx 0.248 \cdot 2\pi$  at  $k \approx 0.405 \cdot 2\pi$  of the Dirichlet cell problem and the

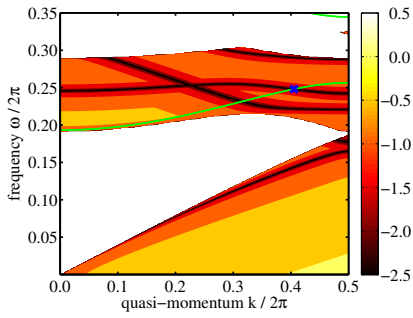


**Fig. 5.1** Magnitude of global distance function  $d_\omega$  in logarithmic scale evaluated on a grid of  $350 \times 500$   $(\omega, k)$ -points. The green lines represent the local Dirichlet eigenvalues, *i. e.* eigenvalues of the local cell problem (3.3a) with homogeneous Dirichlet boundary conditions. The blue cross indicates the location of the eigenvalue for which convergence results are shown in Figures 5.2 and 5.3.

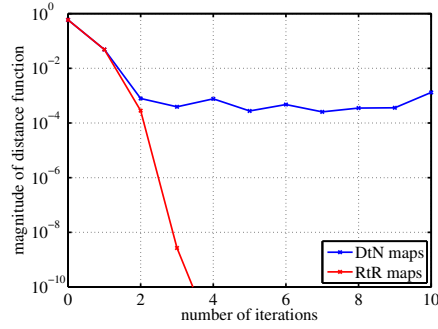


**Fig. 5.2** Convergence of the distance function  $|d_\omega|$  when applying the quasi Newton method with DtN operators (blue) and RtR operators (red) to the computation of the common eigenvalue  $(\omega, k) \approx (0.248 \cdot 2\pi, 0.405 \cdot 2\pi)$  of the Dirichlet cell problem and the non-linear eigenvalue problem (blue cross in Figure 5.1). The start value of the iterative schemes is chosen to be  $\omega^{(0)} = 0.263 \cdot 2\pi$ .

non-linear eigenvalue problem of the PhC wave-guide (blue cross in Figure 5.1). In this example and in all following examples we choose an increment of  $10^{-12}$  in the quasi Newton method for the computation of the first order difference quotient of the global distance function. We compare the convergence of the iterative scheme when applied to the non-linear eigenvalue problem with DtN operators (blue) and with RtR operators (red). While the quasi Newton method with RtR maps converges nicely, we observe that the quasi Newton method with DtN maps converges only until it reaches some error level of order  $10^{-4}$  after two iteration steps. After that the magnitude of the distance function starts to oscillate. This is due to the fact that the local cell problems of the DtN method are ill-posed at the Dirichlet eigenvalues. The closer one comes to such a Dirichlet eigenvalue the larger the error of the local DtN operators becomes.

As alternative to the iterative scheme to solve the non-linear eigenvalue problem, a direct scheme based on a Chebyshev interpolation was introduced in [13]. Now we want to compare the DtN method and the RtR method when such a Chebyshev interpolation is applied to the non-linear eigenvalue problem. Again we aim to compute the common eigenvalue of the local Dirichlet problem and the non-linear eigenvalue problem that is marked as a blue cross in Figure 5.1. We choose the  $k$ -formulation, fix the frequency to  $\omega \approx 0.248 \cdot 2\pi$  and set the  $k$ -interval to  $[0, \pi]$ . In Figure 5.3(a) a comparison of the convergence of the Chebyshev interpolation is shown for the case with DtN operators (blue) and RtR operators (red). We can see that the rate of convergence is for both methods the same, where we have to note that the convergence is not monotone since the Chebyshev nodes are not hierarchical. In Figure 5.3(b) the convergence of the Chebyshev interpolation in  $\omega$ -formulation is shown when choosing the interval  $[0.235 \cdot 2\pi, 0.265 \cdot 2\pi]$  (solid lines) and  $[0.215 \cdot 2\pi, 0.265 \cdot 2\pi]$  (dashed lines). While for the smaller interval both methods converge nicely, we observe that convergence is lost for the larger interval when using the DtN method. The difference

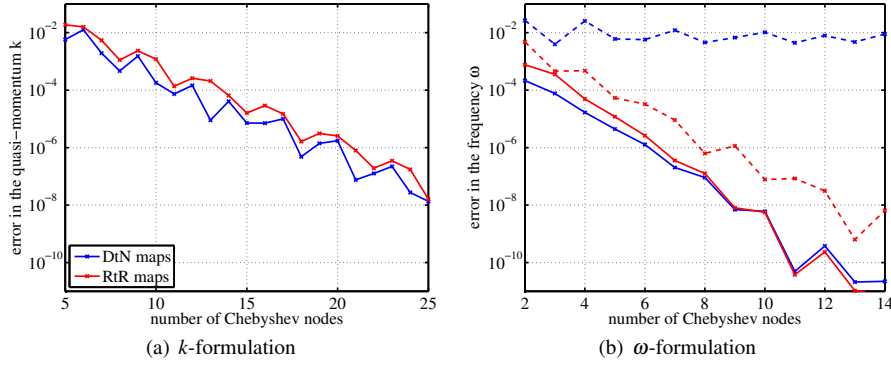


**Fig. 5.3** Convergence of the error for the Chebyshev interpolation to the common eigenvalue at  $(\omega, k) \approx (0.248 \cdot 2\pi, 0.405 \cdot 2\pi)$  of the Dirichlet cell problem and the non-linear eigenvalue problem (blue cross in Figure 5.1) when using DtN operators (blue) and RtR operators (red) in dependence on the number of Chebyshev nodes. In (a) the  $k$ -interval of the interpolation is chosen to be the whole reduced Brillouin zone  $[0, \pi]$ . In (b) the  $\omega$ -interval of the interpolation is chosen to be  $[0.235 \cdot 2\pi, 0.265 \cdot 2\pi]$  (solid lines) and  $[0.215 \cdot 2\pi, 0.265 \cdot 2\pi]$  (dashed lines).

is that the larger interval contains a global Dirichlet eigenvalue. To understand its influence we first need to study the convergence to global Dirichlet eigenvalues, which will be addressed in the following subsection.

## 5.2 Computation of surface modes

In our second example we want to study the computation of surface modes of a semi-infinite periodic medium with homogeneous Dirichlet boundary conditions as described in Section 2.3. We solve the non-linear eigenvalue problem (4.1) in  $C_0$  where we replace the RtR transparent boundary condition (4.1b) on the top boundary  $\Gamma_0^+$  by a homogeneous Dirichlet boundary condition. For comparison, we shall either keep the RtR transparent boundary condition (4.1b) on the bottom boundary  $\Gamma_0^-$  or replace it by a DtN transparent boundary condition as introduced in [13]. Choosing the cell  $C_0$  to be identical to the unit cell  $C_1^-$  of the periodic medium, we end up with a setting for which the frequencies of the surface modes are global Dirichlet eigenvalues, *i. e.* eigenvalues of the infinite half-strip problem (3.1a) with homogeneous Dirichlet boundary condition on  $\Gamma_0^\pm$ . Moreover, we note that for this setting a formulation of the problem on  $\Gamma_0^+$  would be possible. However, in this work we shall use the formulation in the cell  $C_0$  in order to employ the method as introduced for the computation of guided modes in PhC wave-guides, and in order to allow for more general settings (*i. e.*  $C_0$  and  $C_1^-$  are different).

In Figure 5.4 we show the magnitude of the global distance function  $d_\omega$  of the RtR method. Recall that the dark lines correspond to small values of  $|d_\omega|$ , and hence represent surface modes. In Figure 5.5 the real part of the surface mode at  $k = 0.40 \cdot 2\pi$  is plotted. It demonstrates well that surface modes are modes that are guided at the surface and decay exponentially in the periodic medium.

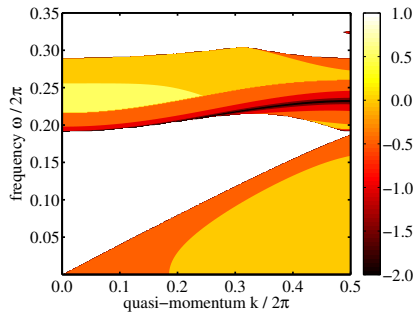


**Fig. 5.4** Magnitude of global distance function  $d_\omega$  in logarithmic scale of surface mode problem evaluated on a grid of  $350 \times 500$   $(\omega, k)$ -points.

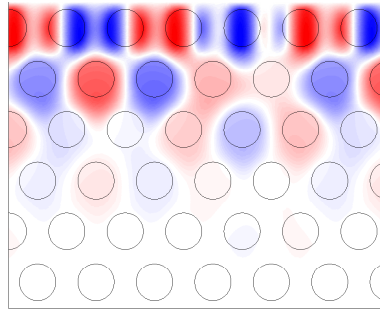


**Fig. 5.5** Real part of the surface mode at  $k = 0.40 \cdot 2\pi$  computed with the RtR method with homogeneous Dirichlet boundary conditions at  $\Gamma_0^+$ .

The convergence curves of the quasi Newton method when applied to the non-linear problem with DtN maps (blue) and with RtR maps (red) is shown in Figure 5.6. Again we observe that the quasi Newton method applied to the problem with RtR maps converges exponentially, while the quasi Newton method applied to the problem with DtN maps only converges until it reaches an error level in  $\omega$  of order  $10^{-5}$ .

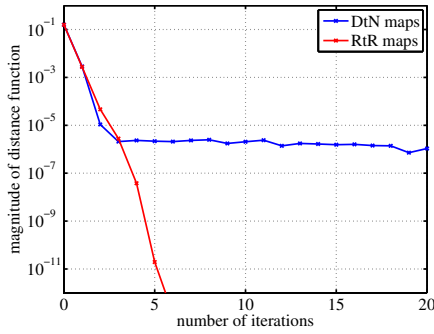


**Fig. 5.6** Convergence of the distance function  $|d_\omega|$  when applying the quasi Newton method with DtN operators (blue) and RtR operators (red) to the computation of the surface mode at  $\omega \approx 0.2173 \cdot 2\pi$  and  $k = 0.45 \cdot 2\pi$ . The start value of the iterative scheme is chosen to be  $\omega^{(0)} = 0.21 \cdot 2\pi$ .

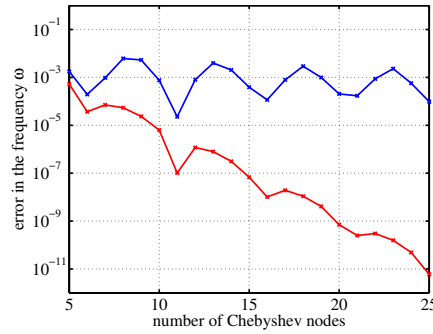


**Fig. 5.7** Convergence of the error in the frequency  $\omega$  for Chebyshev interpolation in  $\omega$ -formulation to the surface mode at  $\omega \approx 0.2173 \cdot 2\pi$  and  $k = 0.45 \cdot 2\pi$  when using DtN operators (blue) and RtR operators (red) in dependence on the number of Chebyshev nodes. The  $\omega$ -interval of the interpolation is chosen to be  $[0.21 \cdot 2\pi, 0.28 \cdot 2\pi]$ .

As in our first example we want to study the Chebyshev interpolation as an alternative to the quasi Newton method and check if it converges even if applied to the problem with DtN maps. The results are shown in Figure 5.7, where we show the error of the Chebyshev interpolation in  $\omega$ -formulation at the quasi-momentum  $k = 0.45 \cdot 2\pi$  and the frequency interval  $[0.21 \cdot 2\pi, 0.28 \cdot 2\pi]$ . We observe that the Chebyshev interpolation applied to the problem with DtN maps does not converge. The Chebyshev interpolation applied to the problem with RtR maps, however, converges, where —

as already described above — the error does not decrease monotonically since the Chebyshev nodes are not hierarchical. The results do not change qualitatively when choosing a smaller  $\omega$ -interval, which helped to restore convergence towards a local Dirichlet eigenvalue, as described in the previous subsection. Moreover, the same results can be obtained when using the  $k$ -formulation of the Chebyshev interpolation. This leaves the question why the Chebyshev interpolation of the problem with DtN maps converges well towards local Dirichlet eigenvalues as long as the interval is chosen small enough, while it does not converge towards global Dirichlet eigenvalues in any case. We address this question in the following subsection where we study the condition number of the system matrix of the non-linear eigenvalue problem and the condition numbers of the DtN matrices.

### 5.3 Condition of system and Dirichlet-to-Neumann matrices

Let  $\mathbf{N}_{\text{DtN}}$  denote the system matrix of the left hand side in Eq. (4.8) where the DtN matrices  $\mathbf{D}_{C_0}^\pm$ , *c.f.* Eq. (4.9), are replaced by the DtN matrices  $\mathbf{D}_{C_0, \text{DtN}}^\pm$  that are obtained using local Dirichlet problems as described in [13] instead of local Robin problems. On the other hand, we shall denote the system matrix in Eq. (4.7) with RtR operators by  $\mathbf{N}_{\text{RtR}}$ .

We recall the example in Section 5.1 of finding guided modes in a PhC waveguide. Since the top and bottom PhCs are equivalent for this configuration we shall only consider the bottom DtN matrix  $\mathbf{D}_{C_0, \text{DtN}}^-$  and denote it by  $\mathbf{D}_{\text{DtN}}$  for simplicity. We study the condition of the system matrices  $\mathbf{N}_{\text{DtN}}$  and  $\mathbf{N}_{\text{RtR}}$  as well as of the DtN matrix  $\mathbf{D}_{\text{DtN}}$  in the second band gap at  $k = 0.4 \cdot 2\pi$ , *c.f.* Figure 5.1. In this band gap the non-linear eigenvalue problem has three eigenvalues (*i.e.* guided modes), and in addition it contains one local Dirichlet eigenvalue (see the green line in Figure 5.1) and one global Dirichlet eigenvalue (see the dark line in Figure 5.4).

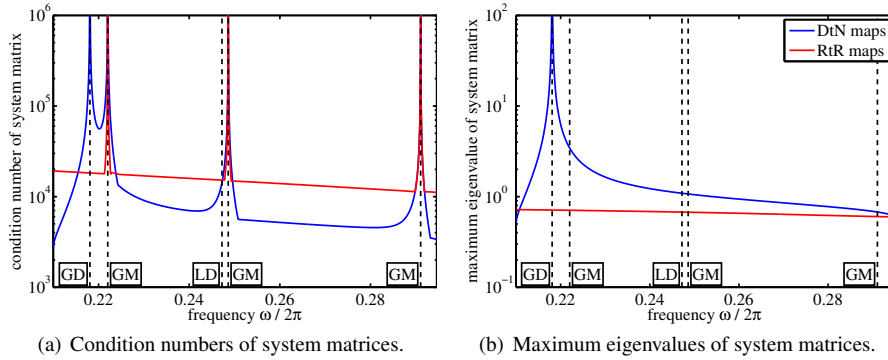


**Fig. 5.8** Condition number (a) and maximum eigenvalue (b) of the system matrix  $\mathbf{N}_{\text{DtN}}$  with DtN maps (blue) and the system matrix  $\mathbf{N}_{\text{RtR}}$  with RtR maps (red) in the second band gap at  $k = 0.4 \cdot 2\pi$ . The vertical dashed line show the frequency of the global Dirichlet eigenvalue (GD), the local Dirichlet eigenvalue (LD) and the frequencies of the guided modes (GM).

In Figure 5.8(a) the condition numbers of the system matrices  $\mathbf{N}_{\text{DtN}}$  and  $\mathbf{N}_{\text{RtR}}$  are shown. The condition numbers increase at the guided modes (dashed lines labeled “GM”) which is due to decreasing minimum eigenvalues of  $\mathbf{N}_{\text{DtN}}$  and  $\mathbf{N}_{\text{RtR}}$  at these eigenvalues of the non-linear operator. Apart from these three peaks, the condition number of the system matrix  $\mathbf{N}_{\text{DtN}}$  with DtN maps also increases in the vicinity of the global Dirichlet eigenvalue (dashed line labeled “GD”), which is due to an increasing maximum eigenvalue of  $\mathbf{N}_{\text{DtN}}$ , see Figure 5.8(b), as it is not an eigenvalue of the non-linear eigenvalue problem. On the other hand, the condition number of the system matrix  $\mathbf{N}_{\text{RtR}}$  with RtR maps as well as its maximum eigenvalue do not increase in the vicinity of the global Dirichlet eigenvalue. In fact, the maximum eigenvalue of  $\mathbf{N}_{\text{RtR}}$  remains almost constant in the complete band gap, see Figure 5.8(b). Note that from Figure 5.8(a) it seems that the local Dirichlet eigenvalue (dashed line labeled “LD”) has no influence on the condition number of  $\mathbf{N}_{\text{DtN}}$ . But we shall study its influence on the condition number in more detail in Figure 5.10(a).

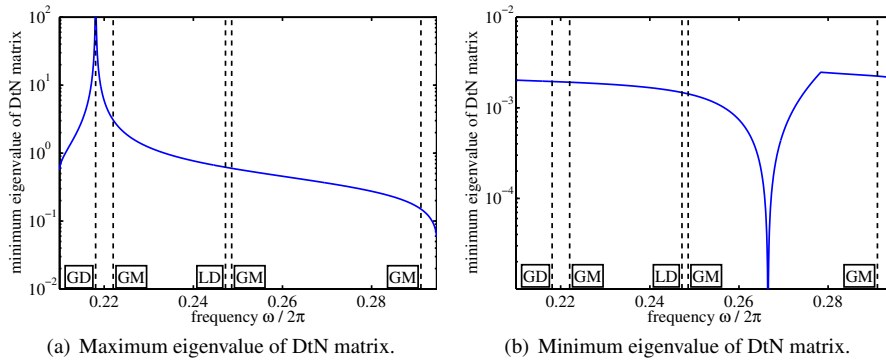


**Fig. 5.9** Maximum eigenvalue (a) and minimum eigenvalue (b) of the DtN matrix  $\mathbf{D}_{\text{DtN}}$  based on local Dirichlet problems in the second band gap at  $k = 0.4 \cdot 2\pi$ . The vertical dashed line show the frequency of the global Dirichlet eigenvalue (GD), the local Dirichlet eigenvalue (LD) and the frequencies of the guided modes (GM).

The increase of the maximum eigenvalue of the system matrix  $\mathbf{N}_{\text{DtN}}$  near the global Dirichlet eigenvalue is due to an increase of the maximum eigenvalue of the DtN matrix  $\mathbf{D}_{\text{DtN}}$  as shown in Figure 5.9(a). While the condition number of the DtN matrix also does not seem to be influenced by the existence of a local Dirichlet eigenvalue, its minimum eigenvalue decreases at some point between the second and third guided mode, see Figure 5.9(b). At this point the PhC half-strip problem with homogeneous Neumann boundary condition has an eigenvalue — a *global Neumann eigenvalue*. However, this decreasing minimum eigenvalue of the DtN matrix does not influence the condition number of the system matrix due to the existence of the Laplace operator, *i. e.* the matrices  $\mathbf{A}_{C_0}(k)$  and  $\mathbf{M}_{C_0}^E$  in Eq. (4.8).

Now let us study the condition number of the system and DtN matrices in a very small vicinity of the local Dirichlet eigenvalue in more detail. Figures 5.10(a) and 5.10(b) show the condition numbers of the two matrices in dependence on the dis-

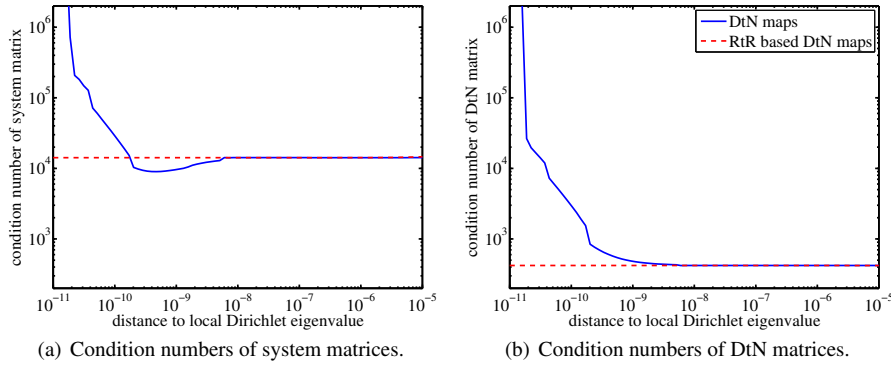


**Fig. 5.10** Condition number of the system matrix  $\mathbf{N}_{\text{DtN}}$  (a) and the DtN matrix  $\mathbf{D}_{\text{DtN}}$  (b) based on local Dirichlet problems (solid blue) and local Robin problems (dashed red) in the vicinity of the local Dirichlet eigenvalue in the second band gap at  $k = 0.4 \cdot 2\pi$ .

tance to the local Dirichlet eigenvalue. The solid lines show the condition numbers of the matrices that are based on local Dirichlet problems and the dashed lines show the condition numbers of the matrices that are based on local Robin problems. While the condition numbers of the matrices related to local Robin problems remain constant in the vicinity of the local Dirichlet eigenvalue, the condition numbers of the matrices that are based on local Dirichlet problems increase dramatically in a small vicinity of the local Dirichlet eigenvalue. Most important is the fact that the increase of the condition number, which explains the convergence problems of the Newton method we observed in Section 5.1, is limited to a very narrow vicinity. Even though the minimum eigenvalues of the local DtN matrices, denoted by  $\mathbf{T}_{ij}^{\pm}$ ,  $i, j = 0, 1$ , in [13], increase in a larger vicinity of the local Dirichlet eigenvalues, the generalized eigenvalue problem related to Eq. (3.24), that is solved for the Dirichlet propagation matrix, can be solved using Matlab's `eig` function without any numerical artifacts up to a very narrow vicinity of the local Dirichlet eigenvalue.

Now we are able to explain why we got convergence towards the local Dirichlet eigenvalue when applying the Chebyshev interpolation in  $k$ -formulation to the problem with DtN maps, and when applying the Chebyshev interpolation in  $\omega$ -formulation for a sufficiently small interval, while we get divergence when the interval is too large. If a Chebyshev node is too close to a global Dirichlet eigenvalue the maximum eigenvalue of the system matrix  $\mathbf{N}_{\text{DtN}}$ , which needs to be evaluated at this node, becomes very large and spoils the solution of the linearized eigenvalue problem. From Figure 5.4 we can see that there does not exist any surface mode, *i. e.* global Dirichlet eigenvalue, in the reduced Brillouin zone  $[0, \pi]$  at the frequency  $\omega \approx 0.248 \cdot 2\pi$ . This means that no matter how large we choose the number  $d$  of Chebyshev nodes, there is never a node too close to a global Dirichlet eigenvalue such that the computation is effected. The same is true if we choose the  $\omega$ -formulation and an  $\omega$ -interval that is sufficiently far away from global Dirichlet eigenvalues. This is the case for the  $\omega$ -interval  $[0.235 \cdot 2\pi, 0.265 \cdot 2\pi]$ , we chose in Figure 5.3(b) (solid lines), while the  $\omega$ -interval  $[0.215 \cdot 2\pi, 0.265 \cdot 2\pi]$  (dashed lines) comprises a global Dirichlet eigen-



1 value. When searching for surface modes the Chebyshev interpolation applied to the  
2 problem with DtN maps has to fail in any case since the interval always contains  
3 a global Dirichlet eigenvalue (since surface modes are global Dirichlet eigenvalues)  
4 and hence, for any sufficiently large number  $d$  of Chebyshev nodes there will be a  
5 node that is too close to the global Dirichlet eigenvalue.  
6

7 Note that this problem also transfers to the computation of (general) guided modes  
8 that are not equal to local or global Dirichlet eigenvalues when using the Chebyshev  
9 interpolation of the non-linear problem with DtN maps in an interval that is not suffi-  
10 ciently far away from global Dirichlet eigenvalues. This makes the application of the  
11 Chebyshev interpolation to the non-linear problem with DtN maps very problematic  
12 as long as we do not have a-priori knowledge about the existence and location of  
13 global Dirichlet eigenvalues.

14 Applying the (quasi) Newton's method to the problem with DtN maps, on the  
15 other hand, only seems to be problematic if the sought guided mode is equivalent to  
16 a local or global Dirichlet eigenvalue.  
17

## 18

## 19 **6 Conclusion**

## 20

21 In this paper we showed the numerical discretization of RtR operators based on lo-  
22 cal cell problems with given Robin data. These operators are then employed for the  
23 exact computation of guided modes in 2D PhC wave-guides and surface modes in  
24 semi-infinite 2D PhCs. The RtR operators and the local Robin problems are well-  
25 defined at all frequencies in band gaps and therefore, they are preferable compared to  
26 DtN operators based on local Dirichlet problems as used in [5, 13]. In numerical ex-  
27 amples we showed that our proposed quasi Newton method converges even if we are  
28 very close to a Dirichlet eigenvalue of the PhC unit cell (local Dirichlet eigenvalue)  
29 or to a Dirichlet eigenvalue of the PhC half-strip (global Dirichlet eigenvalue) where  
30 the method with DtN operators based on local Dirichlet problems does not converge.  
31 Apart from these special cases we could also show that the Chebyshev interpola-  
32 tion of the non-linear problem with DtN operators only converges if the interpolation  
33 interval does not contain and is sufficiently far away from any global Dirichlet eigen-  
34 value. However, those global Dirichlet eigenvalues are normally unknown in advance,  
35 in particular since their computation is only possible with RtR operators, as shown  
36 in this paper. The method with RtR operators, on the other hand, proved to be reli-  
37 able for the computation of guided modes and surface modes no matter if an indirect  
38 method, such as the quasi Newton method, or a direct method, such as the Chebyshev  
39 interpolation, is used to solve the resulting non-linear eigenvalue problem.  
40  
41

## 42

## 43 **References**

## 44

- 45 1. C. Besse, J. Coatléven, S. Fliss, I. Lacroix-Violet, and K. Ramdani. Transparent boundary conditions  
46 for locally perturbed infinite hexagonal periodic media, 2012. arXiv:1205.5345v1.
  - 47 2. J. Coatléven. Helmholtz equation in periodic media with a line defect. *J. Comput. Phys.*, 231(4):1675–  
48 1704, 2012.
  - 49 3. Concepts Development Team. *Webpage of Numerical C++ Library Concepts 2*.  
50 <http://www.concepts.math.ethz.ch>, 2013.
- 51  
52  
53  
54  
55  
56  
57  
58  
59  
60  
61  
62  
63  
64  
65

4. S. Fliss. *Etude mathématique et numérique de la propagation des ondes dans des milieux périodiques localement perturbés*. PhD thesis, École Doctorale de l'École Polytechnique, May 2009.
5. S. Fliss. A Dirichlet-to-Neumann approach for the exact computation of guided modes in photonic crystal waveguides, 2012. arXiv:1202.4928v2.
6. S. Fliss, E. Cassan, and D. Bernier. New approach to describe light refraction at the surface of a photonic crystal. *JOSA B*, 27:1492–1503, 2010.
7. S. Fliss and P. Joly. Exact boundary conditions for time-harmonic wave propagation in locally perturbed periodic media. *Appl. Numer. Math.*, 59(9):2155–2178, 2009.
8. S. Fliss, P. Joly, and J.-R. Li. *Exact boundary conditions for wave propagation in periodic media containing a local perturbation*, chapter 5, pages 108–134. Number 1. 2010.
9. P. Frauenfelder and C. Lage. Concepts – an object-oriented software package for partial differential equations. *Math. Model. Numer. Anal.*, 36(5):937–951, 2002.
10. J. D. Joannopoulos. *Photonic crystals: Molding the flow of light*. Princeton University Press, Princeton, NJ, USA, 2008.
11. P. Joly, J.-R. Li, and S. Fliss. Exact boundary conditions for periodic waveguides containing a local perturbation. *Commun. Comput. Phys.*, 1(6):945–973, 2006.
12. T. Katō. *Perturbation theory for linear operators*. Grundlehren der mathematischen Wissenschaften. Springer, Berlin & Heidelberg, Germany, 1995.
13. D. Klindworth, K. Schmidt, and S. Fliss. Numerical realization of Dirichlet-to-Neumann transparent boundary conditions for photonic crystal wave-guides. Accepted for publication in *Comput. Math. Appl.*, 2013.
14. P. Kuchment. *Floquet theory for partial differential equations*. Birkhäuser, Basel, Switzerland, 1993.
15. J. M. Melenk and S. Sauter. Wavenumber explicit convergence analysis for Galerkin discretizations of the helmholtz equation. *SIAM J. Numer. Anal.*, 49(3):1210–1243, 2011.
16. S. Sauter and C. Schwab. *Boundary element methods*. Springer, Berlin & Heidelberg, Germany, 2011.
17. K. Schmidt and P. Kauf. Computation of the band structure of two-dimensional photonic crystals with *hp* finite elements. *Comp. Meth. App. Mech. Engr.*, 198:1249–1259, 2009.
18. O. Steinbach. On a generalized  $L^2$  projection and some related stability estimates in Sobolev spaces. *Numer. Math.*, 90(4):775–786, 2002.
19. F. Tisseur and K. Meerbergen. The quadratic eigenvalue problem. *SIAM Rev.*, 43(2):235–286, 2001.
20. B. I. Wohlmuth. A mortar finite element method using dual spaces for the Lagrange multiplier. *SIAM J. Numer. Anal.*, 38(3):989–1012, 2001.